

TR- 113 Volume I  
1980



## Comparison of Methods for Determining Soil Hydraulic Characteristics

T.A. Howell  
M.J. McFarland  
D.L. Reddell  
K.W. Brown  
R.J. Newton  
K.B. Humphreys

---

**Texas Water Resources Institute**

---

**Texas A&M University**

RESEARCH PROJECT COMPLETION REPORT

Project Number B-219-TEX

(October 1, 1977 - December 31, 1980)

Agreement Number 14-34-001-8121

IMPROVED WATER AND NUTRIENT MANAGEMENT  
THROUGH HIGH-FREQUENCY IRRIGATION

PRINCIPAL INVESTIGATORS

Terry A. Howell  
Marshall J. McFarland  
Donald L. Reddell  
Kirk W. Brown  
Ronald J. Newton

Volume I: Comparison of Methods for Determining  
Soil Hydraulic Characteristics

CO-INVESTIGATORS

Kathryn Byrd Humphreys  
Terry A. Howell

The work on which this publication is based was supported in part by funds provided by the Office of Water Research and Technology, U.S. Department of the Interior, Washington, D. C., (Project B-219-TEX) as authorized by the Water Research and Development Act of 1978, and the Texas Agricultural Experiment Station.

Contents of this publication do not necessarily reflect the views and policies of the Office of Water Research and Technology, U.S. Department of the Interior, nor does mention of trade names or commercial products constitute their endorsement or recommendation for use by the U.S. Government.

TECHNICAL REPORT NO. 113 VOL. 1  
Texas Water Resources Institute  
Texas A&M University

December 1980

## ABSTRACT

An adequate description of soil moisture movement is necessary for solution of agriculturally oriented problems such as irrigation, drainage and runoff control. Three approaches for determining the hydraulic properties of soil are in situ measurements, laboratory measurements and theoretical models. Field measurements, though representative, have the disadvantages of being costly and time consuming. Laboratory and mathematical processes are more practical but require extensive comparison to field results for evaluation. The purpose of this study was to determine the principle hydraulic properties of a soil of the Norwood Series utilizing the three approaches and to compare the results.

The laboratory method selected was centrifugation (Alemi, et al., 1972). Soil cores were centrifuged and the redistribution of water was measured as change in weight with time. Inconsistent results and limited data obtained with this method, consequently, prevented adequate conclusions from being made.

Hydraulic conductivity was obtained by measurement of hydraulic head and moisture content of the soil profile in situ with tensiometers and neutron probe, respectively. The theoretical procedure utilized water retentivity curves in conjunction with values of saturated hydraulic conductivity for computing hydraulic conductivity as a function of water content. Saturated hydraulic conductivity was measured in the field using Bouwer's (1961) double-tube method. The pressure-water content curves were obtained with disturbed soil samples for 30 to 80 cm depths and with soil cores for 0 to 15 cm

depths using pressureplate extractors. A combination of laboratory and field measured values for these curves was also used for comparison.

The field measurements yielded several relationships between hydraulic conductivity and water content, varying with soil depth. Comparison of calculated values with field data using only the laboratory water retention curves gave mediocre results for the 30 to 80 cm soil depth. However, when the field and laboratory data were combined and the resulting water retention curve was used to calculate hydraulic activity, the correlation was greatly improved. The 0 to 20 cm soil depth showed good results with both curves. Thus, it appears that this theoretical technique is applicable to soils of the type studied, but the accuracy of the calculated values is quite sensitive to the shape of the water retention curve, the saturated water content value and the saturated hydraulic conductivity value. Thus, accurate measurement of these parameters is necessary for its successful use.

## TABLE OF CONTENTS

Chapter		Page
I	INTRODUCTION . . . . .	1
II	LITERATURE REVIEW . . . . .	3
III	EXPERIMENTAL PROCEDURE . . . . .	16
	Measurement of Soil Hydraulic Properties in the Laboratory . . . . .	16
	Pressure Chamber Method . . . . .	16
	Centrifuge Method . . . . .	17
	Measurement of Soil Hydraulic Properties in the Field . . . . .	20
	Double-Tube Method . . . . .	20
	Instantaneous Profile Method . . . . .	22
IV	RESULTS AND DISCUSSION . . . . .	28
	Soil Profile Hydrology . . . . .	32
	Double-Tube Method . . . . .	39
	Laboratory Measurements . . . . .	47
	Centrifuge Measurements . . . . .	56
V	SUMMARY AND CONCLUSIONS . . . . .	63
	Recommendations for Future Study . . . . .	64
	REFERENCES . . . . .	66
	APPENDIX A . . . . .	69

## LIST OF TABLES

Table		Page
1	Texture profile of field site . . . . .	29
2	Saturated conductivities measured with double-tube apparatus . . . . .	45
A-1	Field measurement of bulk density . . . . .	70
A-2	Neutron probe calibration data . . . . .	71
A-3	Soil moisture measured at different depths for various times during drainage . . . . .	73
A-4	Soil-water pressure head (cmH <sub>2</sub> O) measured at different depths for various times during drainage . . . . .	74
A-5	Calculation of hydraulic conductivity from field data . . . . .	75
A-6	Water retentivity values of pressure potential and water content used in the calculation of hydraulic conductivity . . . . .	81
A-7	Double-tube data used for calculation of K <sub>s</sub> . . . . .	86
A-8	Centrifuge data . . . . .	90

## LIST OF FIGURES

Figure		Page
1	Detail of double-tube apparatus showing dimensions, inner tube, outer tube and standpipes. . . . .	12
2	Values of flow factor, F (Bouwer and Jackson, 1974) . .	14
3	Soil core weighing apparatus for centrifuge method . . . . .	19
4	Schematic diagram of plot layout showing dimensions, instrumented section and manometer location. . . . .	23
5	Schematic diagram of instrument layout showing relative positions of neutron access tubes, tensiometers and tensiometer depths . . . . .	24
6	Bulk density profile showing gamma probe data, gravimetric results and texture profile. . . . .	30
7	Calibration curve for neutron soil moisture probe . . .	31
8	Tensiometry showing pressure head versus drainage period for each depth.(smoothed data) . . . . .	33
9	Hydraulic head profiles for different times. (smoothed data) . . . . .	34
10	Soil moisture profiles for different times . . . . .	36
11	Soil moisture for different depths . . . . .	37

## LIST OF FIGURES (Continued)

Figure		Page
12	Volume flux versus time for various depths. . . . .	38
13	Relationship between hydraulic conductivity and water content determined from field measurements for 10-30 cm soil depth . . . . .	40
14	Relationship between hydraulic conductivity and water content determined from field measurements for 40-80 cm soil depth . . . . .	41
15	Relationship between hydraulic conductivity and water content determined from field measurements for 90-120 cm soil depth . . . . .	42
16	Relationship between hydraulic conductivity and water content determined from field measurements for 140-160 cm soil depth . . . . .	43
17	Relationship between hydraulic conductivity and water content determined from field measurements for 170-180 cm soil depth . . . . .	44
18	Saturated hydraulic conductivity versus depth . . .	46
19	Water retentivity determined in the laboratory, 0-15 cm soil depth. . . . .	48
20	Water retentivity determined in the laboratory, 15-55 cm soil depth. . . . .	49
21	Water retentivity determined in the laboratory, 55-90 cm soil depth. . . . .	50
22	Comparison of calculated to measured hydraulic conductivity, 0-25 cm soil depth. . . . .	51
23	Comparison of calculated to measured hydraulic conductivity, 30-80 cm soil depth . . .	53



## LIST OF FIGURES (Continued)

Figure		Page
24	Water retentivity from field data combined with laboratory data, 0-25 cm soil depth. . . . .	54
25	Water retentivity from field data combined with laboratory data, 15-55 cm soil depth . . . . .	55
26	Comparison of calculated to measured hydraulic conductivity, 0-25 cm soil depth. . . . .	57
27	Comparison of calculated to measured hydraulic conductivity, 30-80 cm soil depth . . . . .	58
28	Hydraulic conductivity versus water content determined from centrifuge data for noted soil depths . . . . .	60
29	Comparison of laboratory to field hydraulic conductivity, 0-30 cm soil depth . . . . .	61
30	Comparison of laboratory to field hydraulic conductivity, 40-80 cm soil depth . . . . .	62
A-1	Double-tube data for 5 cm depth . . . . .	87
A-2	Double-tube data for 40 cm depth . . . . .	88
A-3	Double-tube data for 70 cm depth . . . . .	89

## LIST OF SYMBOLS

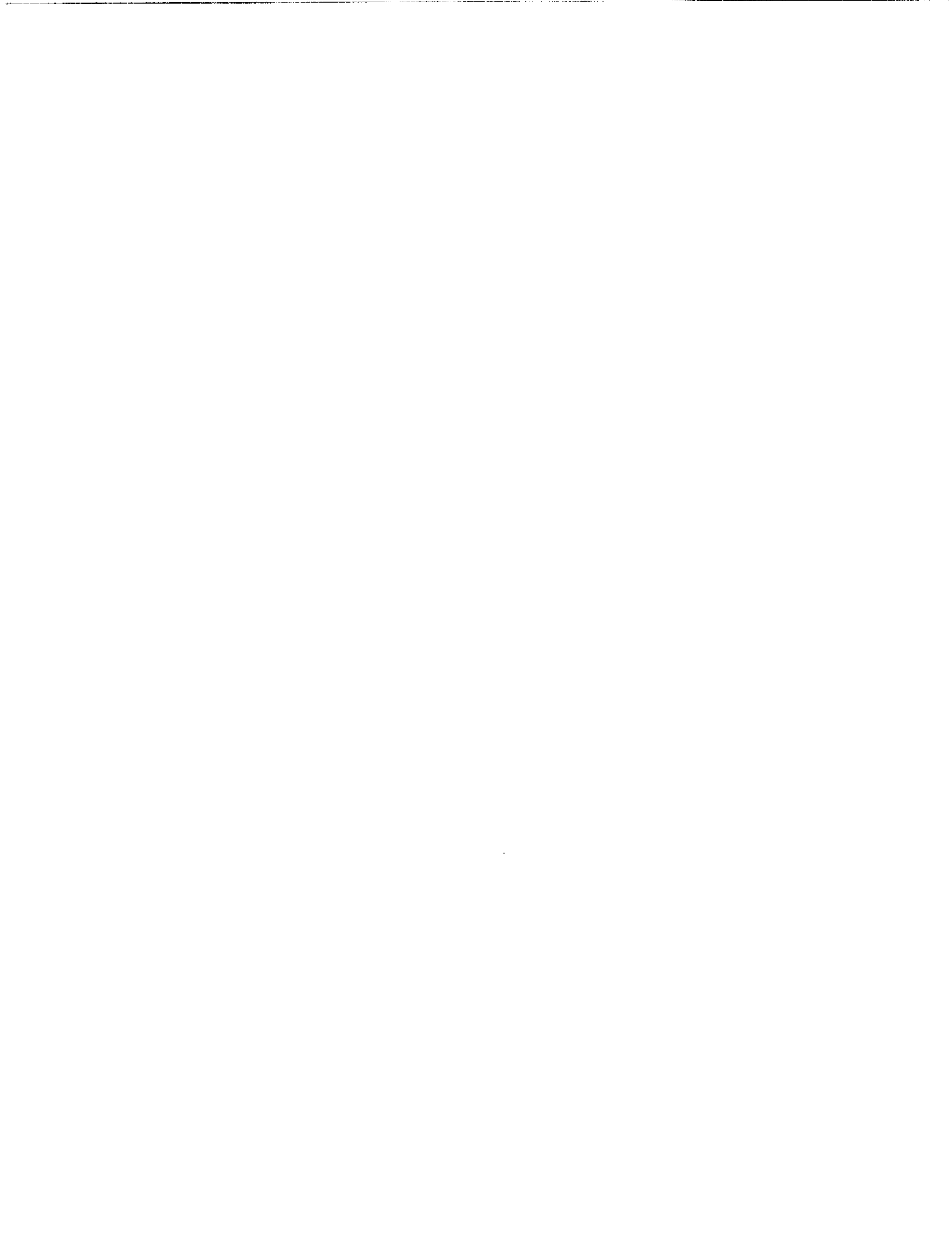
<u>Symbol</u>	<u>Definition</u>
C	Specific water capacity (1/L).
CR	Count ratio, measured/standard.
D	Depth of slowly permeable material beneath auger hole (L).
Db	Bulk density (M/L <sup>3</sup> ).
Dp	Depth of highly permeable material beneath auger hole (L).
Dw	Soil water diffusivity (L <sup>2</sup> /T).
F	Flow factor, dimensionless.
Fcp	Centripetal force per unit mass (L/T <sup>2</sup> ).
H	Total head (L).
HB	Head measured in inner-tube standpipe (L).
HB <sub>1</sub>	Head measured in inner-tube standpipe during outer-tube constant measurement (L).
K	Hydraulic conductivity (L/T).
L	Length of soil core (L).
Lm	Total length of bridge to hold soil core (L).
Q <sub>H</sub>	Flow moving in or out of inner tube due to head difference between tubes (L <sup>3</sup> /T).
R	Radius from center of centrifuge (L).
R <sub>1</sub>	Reaction measured on balance (M).

## LIST OF SYMBOLS (Continued)

<u>Symbol</u>	<u>Definition</u>
Rc	Radius of inner-tube standpipe (L).
Rv	Radius of inner-tube (L).
S	Total porosity (%).
Z	Soil depth (L).
d	Depth of penetration of inner-tube (L).
g	Gravitational acceleration ( $L/T^2$ , $F/M$ ).
h	Pressure head (L) or ( $F/L^2$ ).
hg	Gravitational head (L).
i	Summation index.
j	Summation index.
k	Permeability ( $L^2$ ).
m	Number of water content increments of water retention curve.
n	Summation index.
nm	Number of water content increments of water retention curve from zero to saturation.
p	Particle density ( $M/L^3$ ).
q	Volume flux (L/T).
s	subscript, denotes saturation.
t	Time (T) or subscript denoting time.
z	Distance between points of flow (L).

## LIST OF SYMBOLS (Continued)

<u>Symbol</u>	<u>Definition</u>
$\gamma$	Surface tension (F/L).
$\rho$	Density (M/L <sup>3</sup> ).
$\theta$	Volumetric water content (L <sup>3</sup> /L <sup>3</sup> ).
$\eta$	Viscosity (FT/L <sup>2</sup> ).
$\omega$	Angular velocity (1/T).
$\sigma$	Exponent of $\theta_i/\theta_s$ for Jackson's equation.



## CHAPTER I

### INTRODUCTION

Solutions to problems involving irrigation, runoff control, drainage and water conservation are dependent upon a description of soil moisture movement. With respect to plant water requirements, the water storage capacity of a soil is determined by infiltration, redistribution and drainage processes which also rely on knowledge of soil moisture movement. Three approaches used to determine the relevant hydraulic properties utilized in describing soil moisture patterns are in situ measurements, laboratory processes, and mathematical models.

Field measurements, though more representative of actual conditions, have the disadvantage of being costly and time consuming, whereas laboratory and mathematical processes, though more practical compared to field techniques, require extensive comparison to field results to determine the validity for various soils.

Soil hydraulic characteristics are best described by the relationship between hydraulic conductivity and soil water content. In this study, this relationship will be determined using in situ measurements, with a laboratory technique and by a theoretical procedure. An

evaluation of the laboratory technique and the theoretical procedure will be made by comparing them with field data. Specifically, the objectives of this study were:

1. To determine the unsaturated hydraulic conductivity of a soil in situ using the instantaneous profile method (Watson, 1966, van Bavel, et al., 1968, Hillel, et al., 1972).
2. To determine the pressure head-water content relationship of a soil using the pressure chamber method (Richards, 1947) and to determine the saturated hydraulic conductivity using the double-tube method described by Bouwer (1961). These relationships were then used in a theoretical model developed by Millington and Quirk (1960) and Marshall (1958) as described by Jackson (1972) to predict the relationship between unsaturated hydraulic conductivity versus soil water content for a soil.
3. To determine the unsaturated hydraulic conductivity on soil cores from the field using a simplified centrifugation method described by Alemi, et al., (1976).
4. To compare the results obtained in the field (instantaneous profile) with those acquired in the laboratory (centrifugation) and with the theoretical model (Jackson method).

## CHAPTER II

### LITERATURE REVIEW

Capillary flow was first analyzed by E. Buckingham in 1907 (Richards, 1931). Since then, it has been realized that the relationships between pressure potential versus soil water content and hydraulic conductivity versus soil water content are extremely important to the comprehension of soil water movement.

The theory of water movement in soil is based on Darcy's Law which states that flow is proportional to the hydraulic gradient. The equation representing one dimensional flow in a homogeneous isotropic media can be written:

$$q = -K \frac{dH}{dz} \quad (1)$$

where  $q$  is the volume flux (L/T),  $K$  is the hydraulic conductivity (L/T),  $H$  is the piezometric head (L), and  $z$  is the distance between two points along the axis of the flow (L). The piezometric head is the sum of the gravitational head ( $h_g$ ) and the pressure head ( $h$ ) as follows:

$$H = h_g + h. \quad (2)$$

In unsaturated flow, the components of the flow equation,  $K$  and  $H$ , are both dependent on the water content of the soil. These relationships between soil water content versus hydraulic conductivity or



pressure potential are informative hydrological descriptors of a particular soil and are the primary inputs into most theoretical water balance models. The accuracy of these soil properties has a direct bearing on the validity of the theoretical models; therefore, the method used to determine these relationships should yield accurate and representative results.

Hydraulic conductivity versus water content relationships have been evaluated using both laboratory and field techniques. The reliability of the laboratory procedures is determined by comparison to field measurements. Soil sampling necessary to laboratory procedures is the major reason for discrepancy since the sample size is severely decreased from that in the field and natural environmental factors are absent.

The two approaches generally used to evaluate these relationships in the laboratory are: (1) a steady-state approach and (2) a non-steady-state approach. For steady-state flow, it is necessary that the water content, pressure head and flux remain unchanged with time; whereas, these parameters will vary under unsteady-state conditions.

Most laboratory techniques for determining unsaturated hydraulic conductivity under steady-state conditions are based on the two plate method described by Richards (1931). In this method, the volume flux ( $q$ ) through a soil column is measured volumetrically and  $dH/dz$

is measured with tensiometers. Utilizing Darcy's Law, the hydraulic conductivity (K) is calculated. Childs and Collis-George (1950) used the idea that in a long column of soil ending in a water table there is a zone of uniform water content with no pressure head gradient. Therefore, a known applied volume flux is equal to the hydraulic conductivity because the piezometric head gradient is equal to one.

When solving for unsaturated hydraulic conductivity with unsteady-state conditions, soil water diffusivity is used (Klute, 1965b).

Diffusivity is related to conductivity by:

$$D_w = K \frac{dh}{d\theta} = \frac{K}{C} \quad (3)$$

where  $D_w$  is the soil water diffusivity ( $L^2/T$ ),  $h$  is the pressure head (L),  $\theta$  is the volumetric water content ( $L^3/L^3$ ),  $dh/d\theta$  is the slope of the water characteristic curve (L),  $C$  is the specific water capacity ( $1/L$ ), and  $K$  is the hydraulic conductivity ( $L/T$ ).

Several methods have been proposed for measuring diffusivity (Bruce and Klute, 1956, Gardner, 1956, Doering, 1964). The moment method or centrifugation is one of the more recent approaches (Alemi, et al., 1976). When a core of soil is centrifuged at a constant angular velocity for a long time, the centripetal force can be defined as:

$$F_{cp} = R \omega^2 \quad (4)$$

where  $F_{cp}$  is the centripetal force per unit mass ( $L/T^2$ ),  $R$  is the radius from the center of the centrifuge ( $L$ ), and  $\omega$  is the angular velocity ( $1/T$ ). In this approach a soil core is centrifuged to an equilibrium condition determined by the speed of the centrifuge. The redistribution of soil water is then determined by monitoring the weight change as a function of time along the soil column, which is used for calculation of soil water diffusivity. Assumptions underlying this method are: (1) upon cessation of the centrifuge, soil water pressure head changes as a parabolic function of distance along the soil core, (2) the hydraulic conductivity is constant and (3) a linear relationship exists between water content and pressure head.

Childs and Collis-George (1950) demonstrated that permeability could be predicted from pore size distribution instead of particle size distribution as was previously used. The radius of the largest pores holding water is defined by:

$$r = \frac{2\gamma}{h}, \quad (5)$$

where  $r$  is the pore radius ( $L$ ),  $\gamma$  is the surface tension of water ( $F/L$ ) and  $h$  is the water pressure ( $F/L^2$ ). Permeability as a function of pore radius could also be defined as a function of pressure head. Hydraulic conductivity is related to permeability by:

$$K = \frac{k \rho g}{\eta} \quad (6)$$

where  $K$  is the hydraulic conductivity (L/T),  $k$  is the permeability (L<sup>2</sup>),  $\rho$  is the density (M/L<sup>3</sup>),  $g$  is gravitational acceleration (F/M) and  $\eta$  is the viscosity (FT/L<sup>2</sup>). The calculation of unsaturated hydraulic conductivity was greatly simplified by the use of the water retention curve. Marshall (1958) improved this method by developing the following equation to solve for hydraulic conductivity:

$$K = \frac{30\gamma^2}{\rho g \eta} \left(\frac{\theta}{n}\right)^2 \left[ h_1^{-2} + 3h_2^{-2} + 5h_3^{-2} + \dots + (2n-1)h_n^{-2} \right] \quad (7)$$

where  $K$  is the hydraulic conductivity (L/T),  $\gamma$  is the surface tension of water (F/L),  $\rho$  is the density of water (M/L<sup>3</sup>),  $g$  is the gravitational acceleration (F/M),  $\eta$  is the viscosity of water (FT/L<sup>2</sup>),  $\theta$  is the volumetric water content (L<sup>3</sup>/L<sup>3</sup>),  $n$  is the number of water content increments,  $h$  is the pressure head (L), and 30 is a constant obtained from converting pore radius to pressure head, seconds to minutes and using 1/8 from Poiseuille's equation for stream-line flow. Millington and Quirk (1959, 1960) developed a similar relationship for computation of hydraulic conductivity as shown in the following equation:

$$K = \frac{30\gamma^2}{\rho g \eta} \left(\frac{\theta}{nm^2}\right)^{4/3} \left[ h_1^{-2} + 3h_2^{-2} + 5h_3^{-2} + \dots + (2n-1)h_{nm}^{-2} \right] \quad (8)$$

where  $nm$  is the number of water content increments from zero to saturation and  $K, \gamma, \rho, g, \eta$  and  $\theta$  are as previously defined.

Several investigators have tested these equations by comparing

calculated to measured values of hydraulic conductivity (Jackson, et al., 1965, Kunze, et al., 1968, Green and Corey, 1971, Jackson, 1972) with good results. Millington and Quirk (1960) found that comparison of a relative hydraulic conductivity (the ratio of unsaturated to saturated hydraulic conductivity) calculated from their equation gave satisfactory agreement with measured values. Jackson determined this ratio with a general equation using Eq. 7 (Marshall's) and Eq. 8 (Millington and Quirk's) to be:

$$\frac{K_i}{K_s} = \left( \frac{\theta_i}{\theta_s} \right)^\sigma \frac{\sum_{j=i}^m \left[ (2j + 1 - 2i) h_j^{-2} \right]}{\sum_{j=i}^m \left[ (2j - 1) h_j^{-2} \right]}, \quad (9)$$

where  $K$  is the unsaturated hydraulic conductivity (L/T),  $K_s$  is the saturated hydraulic conductivity (L/T),  $\theta_i$  is the volumetric water content at the  $i$ th increment of the water retention curve ( $L^3/L^3$ ),  $\theta_s$  is the volumetric water content at saturation,  $\sigma$  is 4/3 for the Millington-Quirk equation and 0 for the Marshall equation,  $h$  is the pressure head (L),  $m$  is the total number of increments used in the calculation, and  $j$  and  $i$  are summation indices. Comparison of this equation for both values of  $\sigma$  gave reasonable correlation with measured values.

Jackson determined a value for the exponent ( $\sigma$ ) of  $\theta_i / \theta_s$  by comparing calculated values of hydraulic conductivity using various values of  $\sigma$  with measured values to obtain the best fit. Values of  $\sigma$

ranged from 0.82 to 1.24 for sand and 0.74 was the best fit value for a loam. Jackson concluded that a value of 1 for  $\sigma$  was adequate for use with Eq. 9. The variance in  $\sigma$  values appeared to have a greater effect on the sandy soils than on the loam. The deviation of calculated from measured values occurred in the lower water content range, with little or no change for higher water contents. The disagreement for sandy soils appeared to be because values of smaller water content were easier attained with a sand than with a loam, so data in that region of water content was available for comparison. It seems, from Jackson's data then, that this calculating method would be most applicable to agricultural soils which normally maintain higher water contents and any value of  $\sigma$  used, between 0 and 2, has little effect on final values of calculated hydraulic conductivity.

The measurement of soil hydraulic properties in situ eliminates errors associated with soil disturbance which occurs when collecting soil samples for laboratory tests. When the soil is undisturbed, evaluation of soil water flow properties is more representative of actual processes. The instantaneous profile method is a method developed to evaluate soil flow properties under field conditions. This method was originally developed and tested by Watson (1966) on a laboratory model. van Bavel, et al., (1968) and Hillel, et al., (1972) expanded the application to a field situation. Although this procedure

is not valid when horizontal flow is appreciable, it can be used in heterogeneous or layered soil.

To use this method, evaporation from the soil surface is prevented and the soil profile is monitored for changes in soil water content and pressure head while undergoing drainage. Changes in soil water content are obtained with a neutron moisture probe (van Bavel, et al., 1963) and the changes in pressure head are measured with numerous tensiometers located throughout the soil profile (Richards, 1965). The volume flux ( $q$ ) is determined from each soil layer using the water content data and the gradient in hydraulic head ( $dH/dz$ ) for each soil layer is determined from the tensiometer data. The hydraulic conductivity for each soil layer is then determined from Darcy's Law ( $K=q/dH/dz$ ). Thus, one of the principle soil hydraulic properties, the dependence of hydraulic conductivity on water content, is determined. This method is associated with the desorption process only.

The range of water contents measured in this method is limited because of the drainage process. Consequently, the hydraulic conductivity and pressure potential as functions of water content are restricted to this narrow range. One method of increasing the water content range is to include evaporation, but boundary conditions become difficult to define. Another solution is to investigate laboratory or theoretical techniques which would adequately describe the field properties. Good correlation with field results is basic for

extrapolation of field data to lower water contents.

Several procedures are available for determining saturated hydraulic conductivity under field conditions (Bouwer and Jackson, 1974). The procedures for measuring saturated hydraulic conductivity above a water table include the shallow well, pump-in, cylinder permeameter and double-tube. The double-tube method considers the geometry of the flow system.

The double-tube method consists of two concentric cylinders with standpipes installed in the field and filled with water as shown in Fig. 1 (p. 12). When saturation is attained, the rate of water level change in the inner tube is measured under two conditions. In condition 1, the head in the outer tube is kept constant and under condition 2 the head in the outer tube is manipulated to maintain an equal head with the inner tube. The water level change in the inner tube represents the net flow in or out of the inner tube. This net flow consists of movement between the tube within the soil ( $Q_H$ ) plus the actual intake of water by the soil.

When the two head change measurements are plotted as head versus time on the same graph, the distance between the two curves at time  $t$  is:

$$\Delta HB = \int_0^t \frac{Q_H}{\pi R_V^2} dt \quad (10)$$

where  $\Delta HB$  is the head difference between the inner and outer tubes



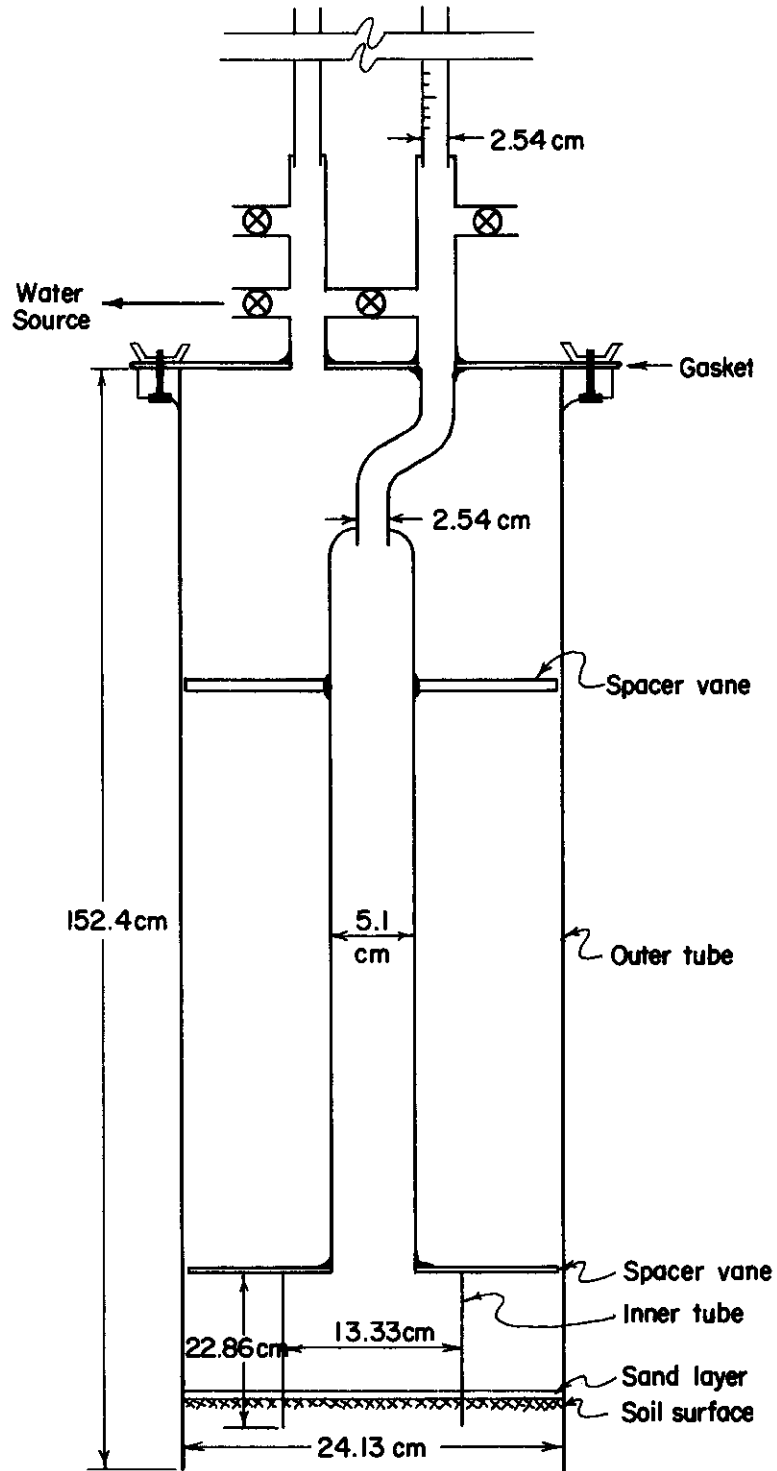


Fig. 1. Detail of double-tube apparatus showing dimensions, inner tube, outer tube and standpipes.

attimet (L),  $Q_H$  is the flow rate leaving or entering the inner due to a difference in head between the tubes ( $L^3/T$ ) and  $R_v$  is the radius of the inner tube standpipe (L).

Bouwer (1961) shows the development of the flow factor which is dependent on soil hydraulic conductivity, system geometry and difference in head between the tubes, i.e.:

$$F = \frac{Q_H}{\pi K_s \Delta H B R_c} \quad (11)$$

where  $F$  is the flow factor (dimensionless),  $R_c$  is the radius of the inner tube (L),  $K_s$  is the saturated hydraulic conductivity ( $L/T$ ), and the other variables are as defined in Eq. 10. A graphical solution of  $F$  as a function of  $D/R_c$ ,  $d/R_c$  and  $D_p/R_c$  was developed by Bouwer (1961), and is reproduced in Fig. 2 (p. 14) from Bouwer and Jackson (1974). In Fig. 2,  $D$  is the depth of the slowly permeable material beneath the auger hole (L),  $D_p$  is the depth of the highly permeable material below the auger hole (L), and  $d$  is the depth of penetration of the inner tube into the bottom of the auger hole (L). For values of  $D > 3R_c$  and  $D_p > 3R_c$ , the curves in Fig. 2 are similar. Thus, for a relatively uniform soil with a large depth either graph could be used. If Eq. 11 is substituted into Eq. 10, a solution for saturated hydraulic conductivity  $K_s$  is:

$$K_s = \frac{HB \int_0^t R_v^2}{FRc \int_0^t HB_1 dt} \quad (12)$$

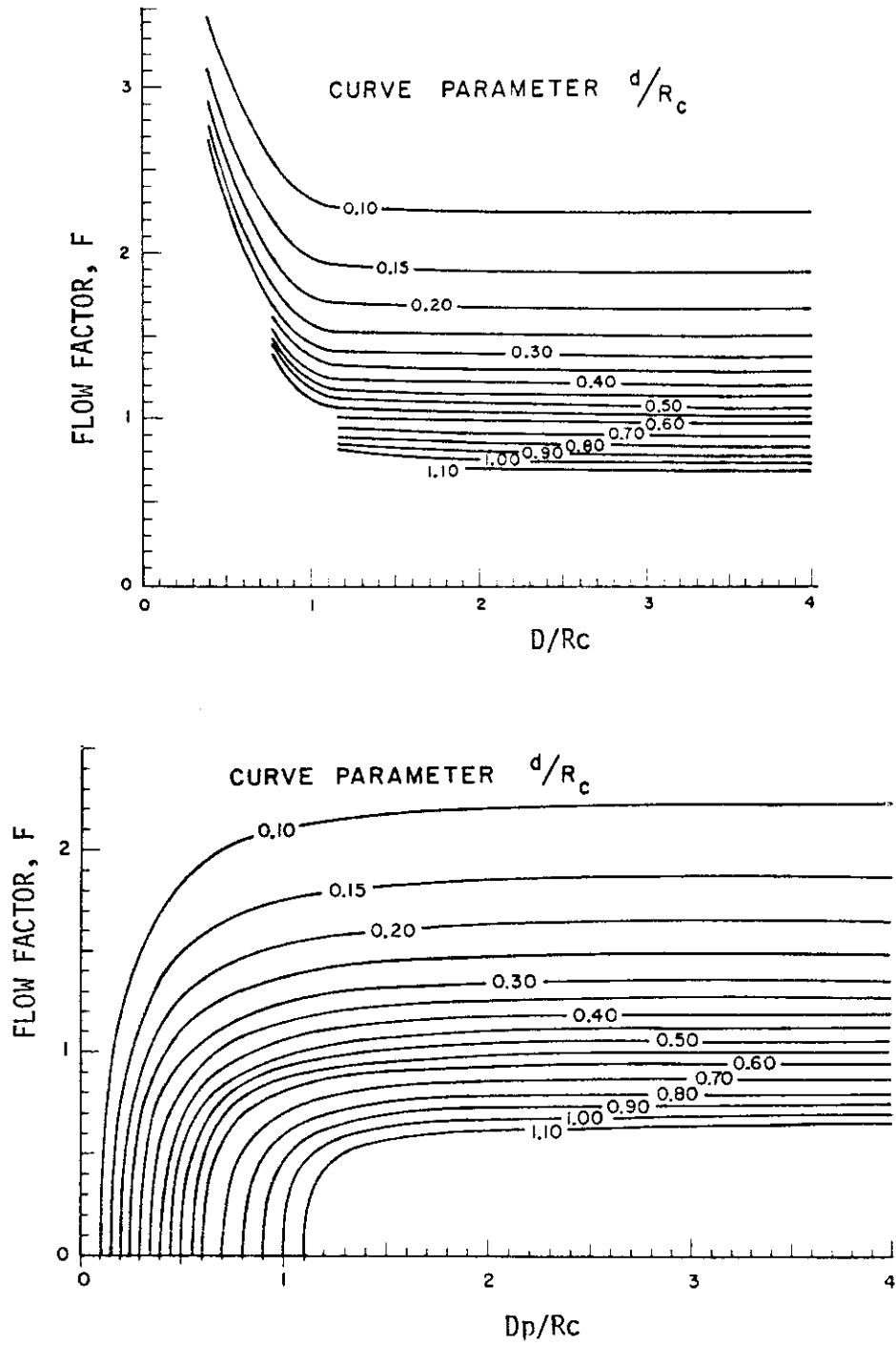


Fig. 2. Values of Flow Factor,  $F$  (Bouwer and Jackson, 1974).

where  $\int_0^t HB_1 dt$  is the area under the head-time curve when the water

level in the outer tube is kept constant (LT) and other variables are as defined in Eqs. 10 and 11.

The capability of accurately predicting water movement within the soil profile has been the object of extensive research. Measurements of these properties in situ yield representative results but are time consuming and expensive. Numerous methods for determining soil hydraulic properties have been developed to facilitate the process, yet maintain the desired accuracy. A few of these methods were described in the above discussion. Although these techniques have been tested on specific soils, the diversity of elements in field situations which affect soil hydraulic properties are cause for additional experimentation.



CHAPTER III  
EXPERIMENTAL PROCEDURE

Measurement of Soil Hydraulic Properties in the Laboratory

Pressure Chamber Method

The water retention properties of the soil were obtained in the laboratory using the pressure chamber method (Richards, 1947). The equipment for this test consisted of six pressure chambers (Soil Moisture Extractor, Cat. No 1 700-2, Soilmoisture Equipment Corp.) attached to pressure regulators which maintain a constant predetermined pressure within each chamber. Porous, ceramic plates, designed to fit within each chamber were used to hold the soil samples and allow water to move out of the samples, through the plate, and into a rubber membrane underneath the bottom side of the ceramic plate. To maintain atmospheric pressure on the bottom side of the ceramic plate, a rubber hose ran from the inside of this membrane to outside the extractor.

Loose soil samples were obtained with a soil auger in the field from soil depths of 15-55 cm and 55-90 cm. A volumetric sampler was utilized to acquire soil cores from the 0-15 cm depth. The loose soil was poured into

---

The use of trade names in this study does not imply endorsement by Texas A&M University.

plastic rings (5 cm diameter, 2 cm length) on each ceramic plate; the soil cores were left in the original volumetric rings (5.7 cm diameter, 6 cm length) and placed on the ceramic plates. They were left standing in water until the soil was saturated. The ceramic plates were then placed inside the pressure chambers and pressures ranging up to 1500 kPa were applied. Specifically, the pressures applied were 10 kPa (.1 bar), 33 kPa (.33 bar), 67 kPa (.67 bar), 100 kPa (1 bar), 200 kPa (2 bar), 500 kPa (5 bar), 1000 kPa (10 bar) and 1500 kPa (15 bar). Allowing four days for the soil water content to reach equilibrium with the applied pressure, the soil samples were removed and soil water contents were determined gravimetrically. Bulk densities, which were previously determined in the field with a volumetric sampler, were used to calculate the volumetric water content from the gravimetric water contents. The pressures applied to the pressure chambers were then plotted versus the resulting volumetric water contents to yield the pressure potential versus volumetric water content function for each soil depth increment.

#### Centrifuge Method

The unsaturated hydraulic conductivity was determined from diffusivity values obtained using a centrifugation technique described by Alemi, et al., (1976). Fifteen soil cores were obtained from the field using a volumetric sampler with brass cylinders 5.7 cm in

diameter and 6 cm in length. Immediately after taking the soil samples, both ends were sealed with parafin film, a rubber gasket, and plastic end caps to prevent any water loss. Simultaneous soil samples were taken from each location to determine the gravimetric water contents.

Each soil core was centrifuged (International Centrifuge, Size 1, Type SB) for periods of at least 60 minutes at speeds ranging from 600 to 800 rpm. A plexiglass bridge, with one end on an analytical balance and the other on an adjustable stand, was devised for measuring the re-distribution of water within the soil core as shown in Fig. 3 (p. 19). Upon cessation of the centrifuge operation the soil core was placed on the bridge with the dry end towards the balance, and the rate of weight change was measured with the analytical balance. The resulting weight was plotted versus the corresponding time. The equation:

$$R_1(t) = R_1(\infty) - \frac{96 R_1(\infty) - R_1(0)}{\pi^4} \sum_{j=1}^{\infty} \frac{1}{(2j-1)^4} \exp\left[-\frac{(2j-1)^2 \pi^2 Dwt}{L^2}\right] \quad (13)$$

was graphed as  $R(t)$  versus  $t$  for various values of  $D$ , where  $R_1(t)$  is the reaction measured on the balance at a specific time ( $M$ ),  $R_1(\infty)$  is the balance reaction at  $t=\infty$  ( $M$ ) and is obtained from the data plot,  $R_1(0)$  is the balance reaction at  $t=0$  ( $M$ ) and is obtained from the data plot,  $L$  is the length of the soil core ( $L$ ),  $t$  is time ( $T$ ), and  $Dw$  is the soil water diffusivity ( $L^2/T$ ). Diffusivity is determined by laying the plot of weight versus time over the plots of  $R_1(t)$  versus  $t$  and  $Dw$  until a



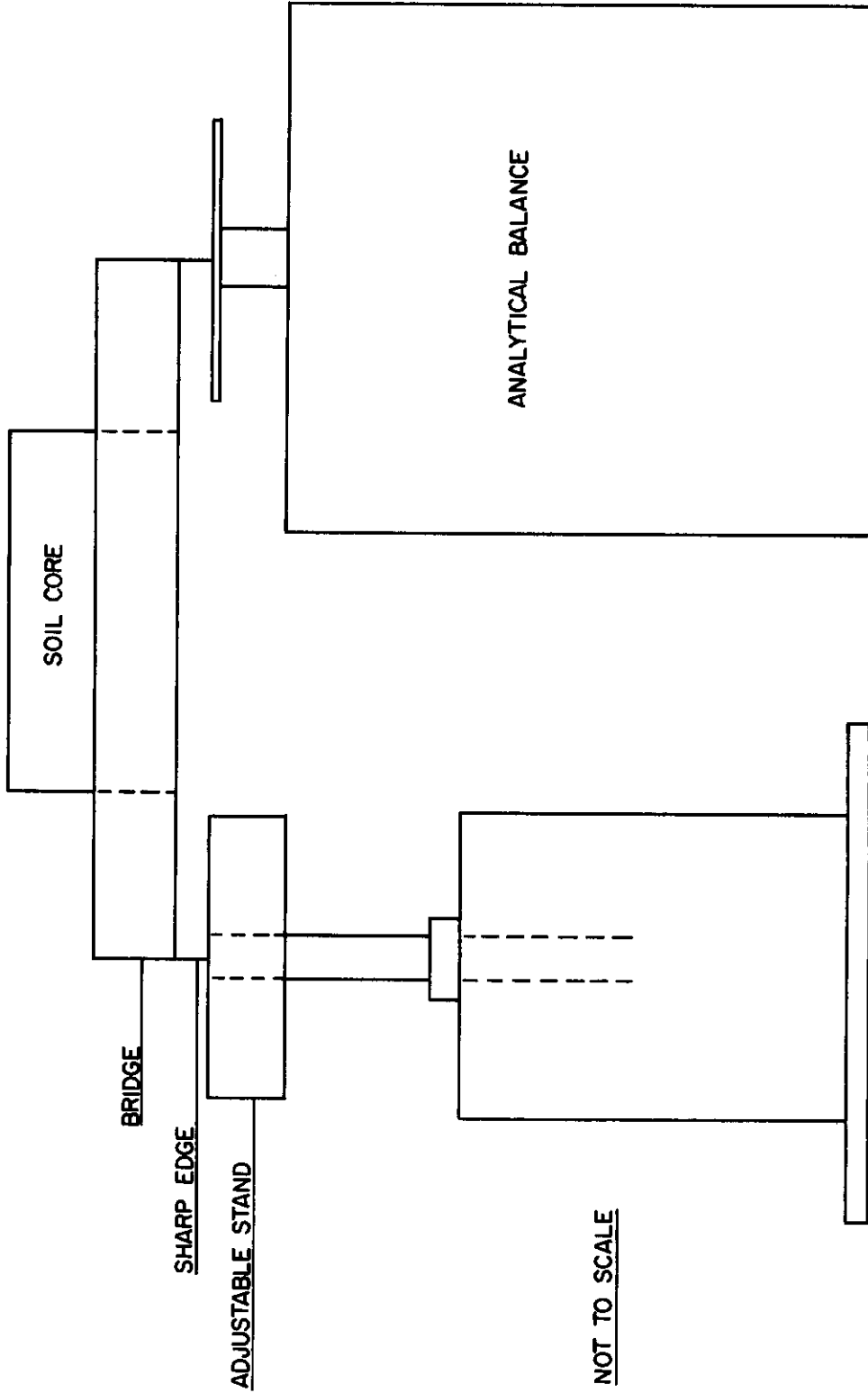


Fig. 3. Soil core weighing apparatus for centrifuge method.

match is achieved. When the two curves match,  $D_w$  is equal to the resulting value on the match curve. After a diffusivity was determined unsaturated conductivity ( $K$ ) was calculated from Eq. 3,  $D_w = K \frac{dh}{d\theta}$ , and  $\frac{dh}{d\theta} = \frac{48gLm}{\rho R \omega^2 L^2 V(4+LR^{-1})} \frac{R_1(\infty) - R_1(0)}$  where  $g$  is the gravitational acceleration ( $L/T^2$ ),  $L_m$  is the length of the bridge ( $L$ ),  $\rho$  is the density of water ( $M/L^3$ ),  $\omega$  is the constant angular velocity of the centrifuge ( $1/T$ ),  $L$  is the length of the soil core ( $L$ ),  $V$  is the bulk volume of the soil core ( $L^3$ ),  $R$  is the radial distance from the center of the centrifuge to the inside edge of the soil core sample, and  $R_1(\infty)$ ,  $R_1(0)$  are as previously defined.

## Measurement of Soil Hydraulic Properties in the Field

### Double-Tube Method

The method selected for measuring saturated hydraulic conductivity was the double-tube method (Bouwer, 1961). The equipment required for this procedure was a double-tube apparatus, water tank and hole cleaner. The outer tube on the double-tube apparatus was made of aluminum tubing (24.23 cm I.D., 152.40 cm length) with a 1.27 cm bottom edge beveled inward. The inner tube was made of iron pipe (13.34 cm I.D.) connected by couplings and reducers to the inner tube standpipe (see Fig. 1., p. 12). The standpipes were made of 2.54 cm plexiglass tubing with a meter stick attached to each.

The hole cleaner was made of a 24 cm diameter wooden plate, with grooves 1.2 cm apart, attached to a metal plate of equal diameter. Metal strips were hammered into the grooves and left protruding 2 cm. When pushed into the soil surface, soil would become entrapped between the blades and be sheared away from the soil surface.

The double-tube method allows the saturated hydraulic conductivity to be measured at various depths. Saturated hydraulic conductivity was determined at depths of 10, 40 and 70 cm. The bottom of each hole was leveled and the hole cleaner was used to clear the disturbed portion of the soil surface. A sand layer, about 2 cm deep, was placed in the bottom of the hole to avoid disturbing the soil surface. The outer tube was put in the hole and forced down about 5 cm below the bottom of the hole. The water was then added, avoiding any soil surface disturbance. The inner tube was placed inside the outer tube when enough time had elapsed to assure saturation and was forced down at least 3 cm below the bottom of the hole. The inner tube was attached to the standpipe and the top plate was secured to make a watertight seal. The valve connecting the standpipes was turned off following simultaneous filling of the standpipes.

Two sets of measurements were necessary for determining the hydraulic conductivity at each depth. The first was the rate of water level change in the inner tube while the water level in the outer tube

was kept at a constant head. The second was a measurement of the change in water head within the inner tube while the head in the outer tube was manipulated to move simultaneously with the head in the inner tube. Saturated hydraulic conductivity was determined from Eq. 12,

$$K_s = \frac{HB_t Rv^2}{F R_c \int_0^t HB_1 dt}$$

#### Instantaneous Profile Method

The purpose of measuring the soil hydraulic properties in situ is to eliminate errors associated with disturbing the soil by sampling and to maintain natural conditions. The procedure used for these measurements was described by Hillel, et al., (1972). The tilled field plot was a bordered 2x2 m section surrounded by a 1.5 m buffer area as shown in Fig. 4 (p. 23). The borders were made of 4x30 cm lumber buried halfway into the soil.

The instrumentation consisted of two neutron access tubes and twenty tensiometers with mercury manometers. The tensiometers were situated at 10 cm depth increments with maximum depth at two meters. The tensiometers were at least 30 cm from each other and 50 cm from the neutron access tubes, as suggested by Hillel, et al., (1972), (Fig. 5, p. 24).

The neutron access tubes were made from 3.81 cm I.D. thin walled aluminum tubing with neoprene stoppers at both ends to protect the

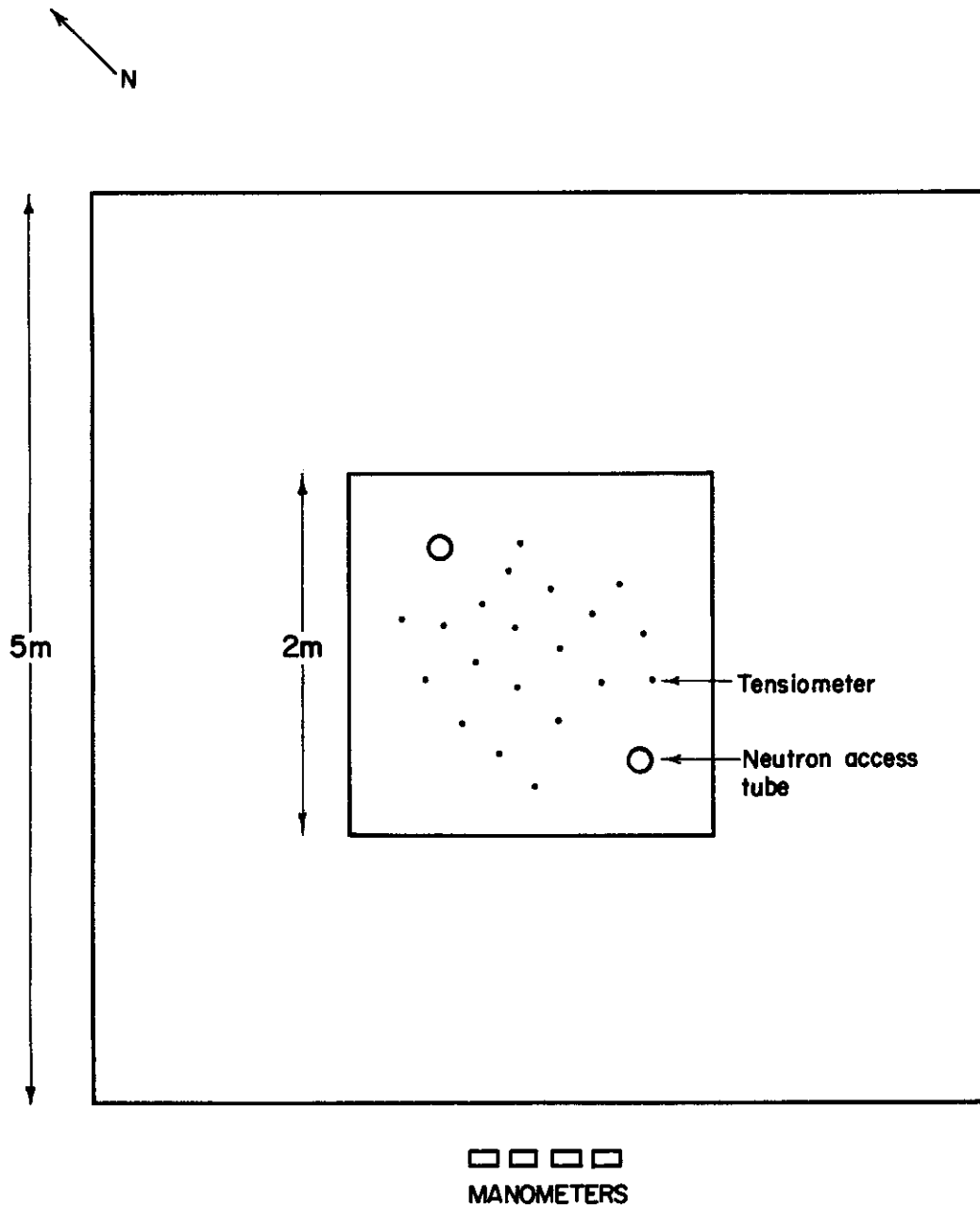


Fig. 4. Schematic diagram of plot layout showing dimensions, instrumented section and manometer location.

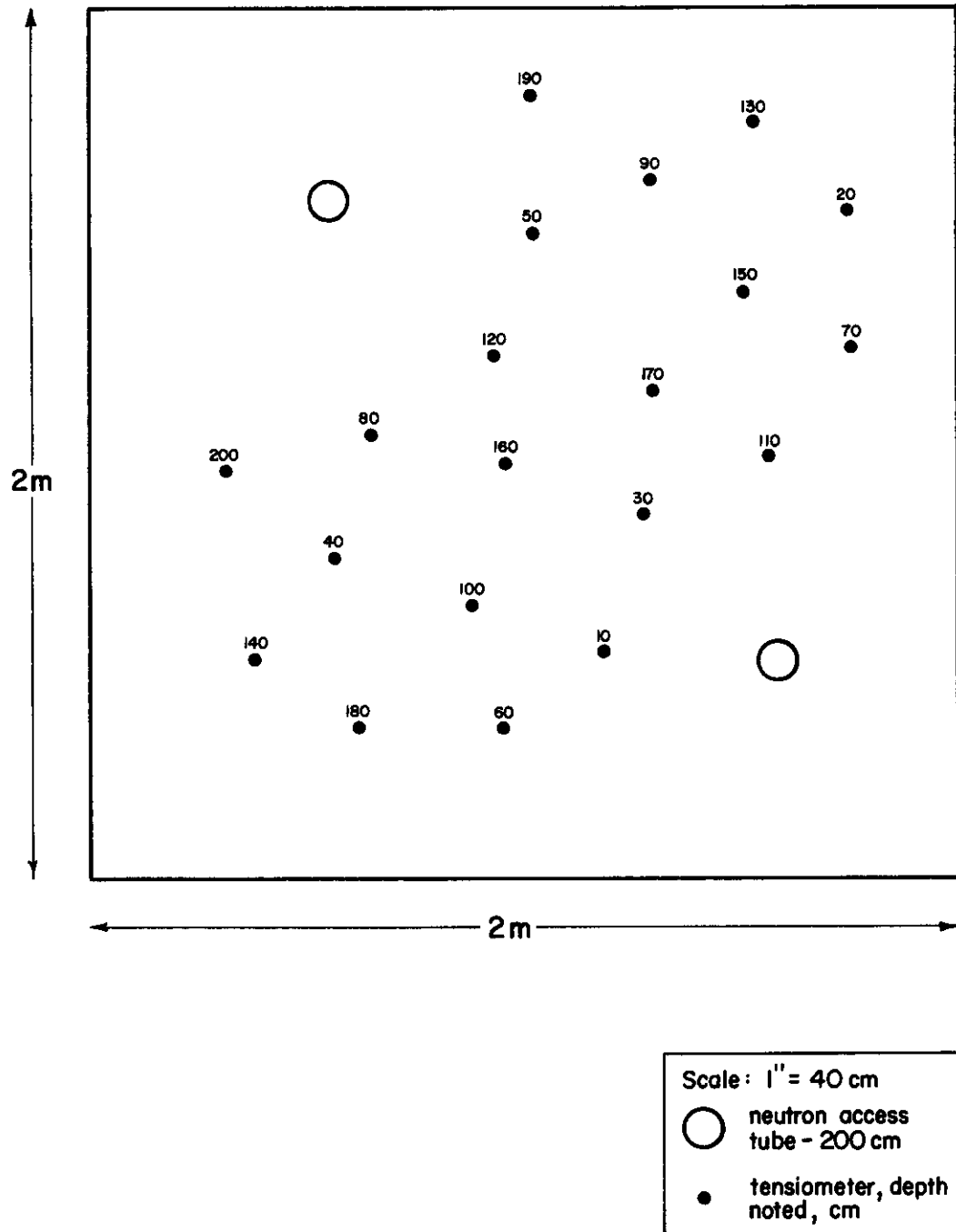


Fig. 5. Schematic diagram of instrument layout showing relative positions of neutron access tubes, tensiometers and tensiometer depths.

inside. Moisture measurements were taken with a neutron soil moisture meter (Model 105A Depth Moisture Probe, Model 600 Scalar, Troxler Electronics Laboratories). Three one-minute standard counts were obtained prior to and following each set of soil moisture readings while the neutron probe was inside the shield and wooden box on the soil surface. The standard counts for each set of data were averaged and divided into the soil moisture counts to obtain a count ratio. Several neutron access tubes were inserted outside the field plot for calibration purposes. Following neutron measurements at known depths, soil samples were taken at equivalent depths with a volumetric sampler to obtain bulk density and gravimetric water content for determining volumetric water content. A correlation was computed for the count ratio and the calculated volumetric water contents. To obtain a wider range of water contents than was available in the field, areas surrounding selected access tubes were irrigated. Bulk density readings in the plot were obtained with a depth density gauge (Model 1352 SN108, Troxler Electronics Laboratories).

The tensiometers were constructed from 1.27 cm I.D. PVC pipe. Porous ceramic cups (Soilmoisture Equipment Co., Cat. No. 2105-1) 0.6 cm O.D. and 2 cm in length were glued to one end of the pipe with epoxy and a small hole was drilled near the other end to allow passage

of a small nylon tube which ran from inside the tensiometer to a reservoir of mercury to become the manometer. Epoxy secured the nylon tubing to the pipe. To install the tensiometer, holes were augered in the soil to the desired depth, the tensiometer was pushed into the soil, and the manometers were installed (Soilmoisture Equipment Corp., Single Manometer Kit, Model 2300). Each tensiometer was maintained with distilled water and checked for air bubbles daily. One tensiometer at the 160 cm depth was faulty after installation in the field.

The plot was initially saturated and the resulting drainage period was monitored. To assure an even distribution of water and minimal soil disturbance during the saturation phase, a 6 mil polyethylene sheet with holes punched in a 10 cm grid pattern was used to cover the plot prior to saturation. A total of 102 cm of water was applied over a one-week period. Evaporation was minimal due to the climactic conditions.

Following the final application of water, the plot was covered with a black polyethylene sheet to prevent plant growth and evaporation. A third transparent sheet was also added. In addition, a polyethylene covered wooden shelter was constructed to cover the 2.2 m plot. The shelter protected the tensiometers, insured that rainfall would not reach the ground and aided in thermal insulation. The top was hinged for easy access to the tensiometers and neutron access tubes.

Neutron readings were started when the final water application



was estimated to have infiltrated. These readings were taken at 10 cm depth increments every two to four hours the first two days, twice per day the following four days, and daily for the following 40 days. Tensiometer readings were taken simultaneously with the soil moisture measurements.

## CHAPTER IV

### RESULTS AND DISCUSSION

The field site was located in the center of field 29 on the Texas A&M University farm. The soil was of the Norwood Series, Typic Udifluent. Using the pipette method of Day (1965) and a sieve analysis, a particle size distribution was obtained for each soil depth and then used to define the soil textural profile. The soil was predominately a silt loam, but silty clay loam dominated the top 20 cm of the soil profile and a thin layer of silty clay loam also occurred at a depth of 160 cm. Despite the general classification, a high clay content (above 24%) existed in the top 30 cm and again at the 120 cm depth as shown in Table 1 (p. 29).

The bulk density of the soil profile, obtained with a gamma density probe and a volumetric soil sampler, varied with depth as shown in Fig. 6 (p. 30). The values of bulk density decreased from 1.59 g/cm<sup>3</sup> at the soil surface to 1.45 g/cm<sup>3</sup> at a depth of 70 cm; and then increased to 1.65 g/cm<sup>3</sup> at the 120 cm depth.

Results from the neutron probe calibration procedure, described earlier, are presented in Fig. 7 (p. 31) as count ratio versus volumetric water content. Two curves were obtained; one curve for the 10 cm soil depth and another for all depths greater than 10 cm. The 10 cm depth calibration curve accounted for the loss of fast neutrons at

TABLE 1

## Texture Profile of Field Site

Depth	% Sand	% Silt	% Clay	Textural Class
0-15	6.40	61.84	31.76	Silty clay loam
15-25	4.00	69.86	26.14	Silt loam
25-35	9.32	74.54	16.14	Silt loam
35-55	10.55	76.84	12.58	Silt loam
55-85	32.20	55.66	12.14	Silt loam
85-95	14.80	73.81	11.39	Silt loam
95-105	23.60	66.16	10.24	Silt loam
105-115	6.95	75.79	17.26	Silt loam
115-145	4.20	71.21	24.59	Silt loam
145-155	10.00	70.00	20.00	Silt loam
155-165	1.75	58.23	40.02	Silty clay
165-185	30.00	56.00	14.00	Silt loam

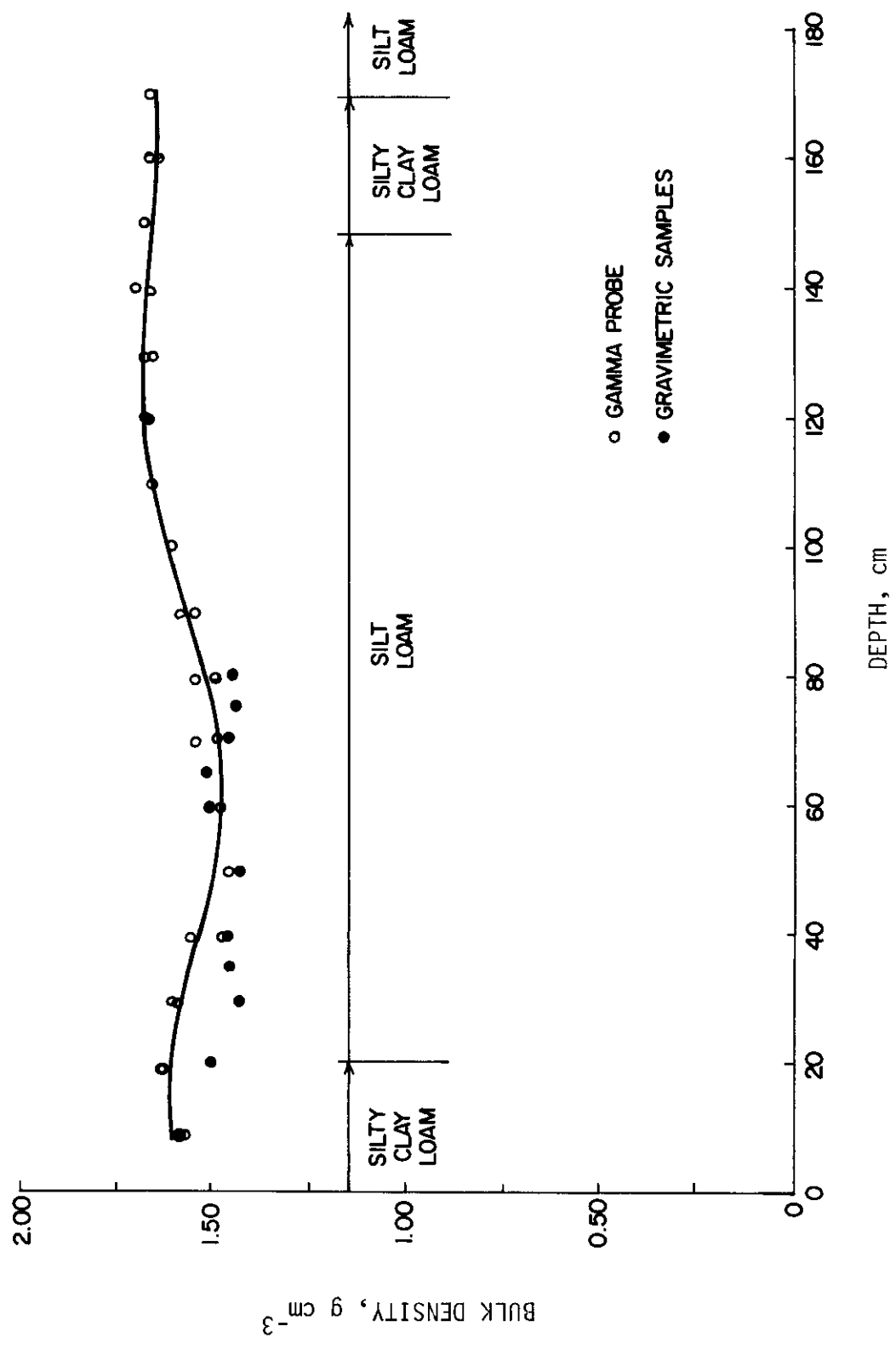
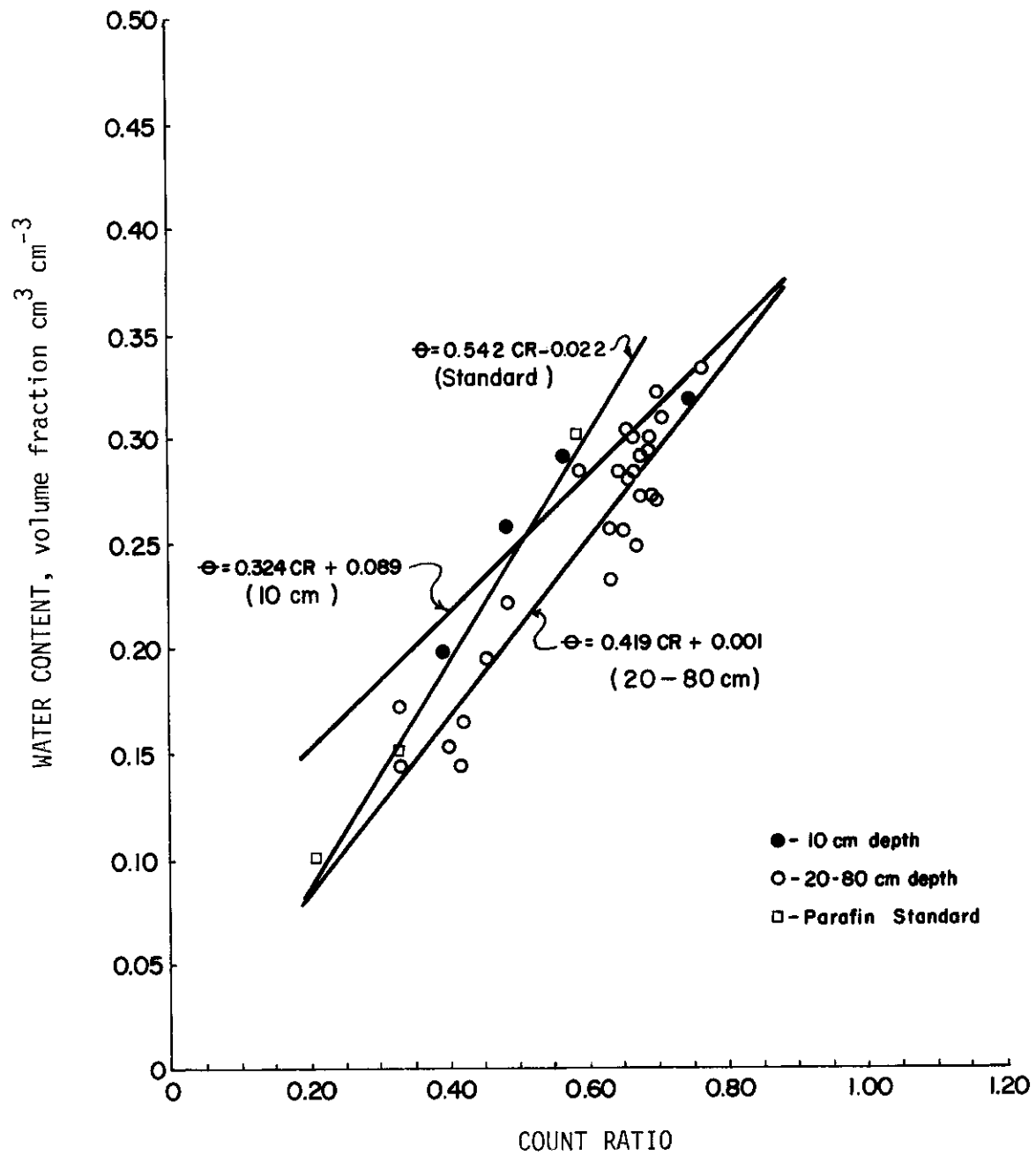


Fig. 6. Bulk density profile showing gamma probe data, gravimetric results and texture profile.



Calibration curve for neutron soil moisture probe.

the soil surface. A lower neutron count reading was obtained for an equivalent water content in the 0 to 15 cm layer as compared to all depths greater than 15 cm. This is demonstrated by the higher intercept value for the 0 to 15 cm curve. Also, the radius of influence increases as the water content decreases causing a greater loss of fast neutrons which results in a lower slope for the 0 to 15 cm layer. Accuracy of soil water content measurements obtained with the neutron probe is limited by the accuracy of the gravimetric soil water contents used to develop the calibration curves.

#### Soil Profile Hydrology

During the first few days of data collection, fluctuations in the tensiometer manometer readings were observed. These fluctuations were caused in part by temperature variations, since the readings were not taken at the same time each day. After the first few days, all readings were taken at 8 a.m. The tensiometer readings were referenced to the soil surface, yielding hydraulic head measurements. Pressure head was calculated by subtracting the depth of the respective tensiometer from the referenced values. The pressure potential for each tensiometer depth is shown in Fig. 8 (p. 33) and the hydraulic head profile for various times is plotted in Fig. 9 (p. 34).

A discontinuity in the average hydraulic head occurred in the 90 to 100 cm depth range. Slopes in hydraulic head averaged

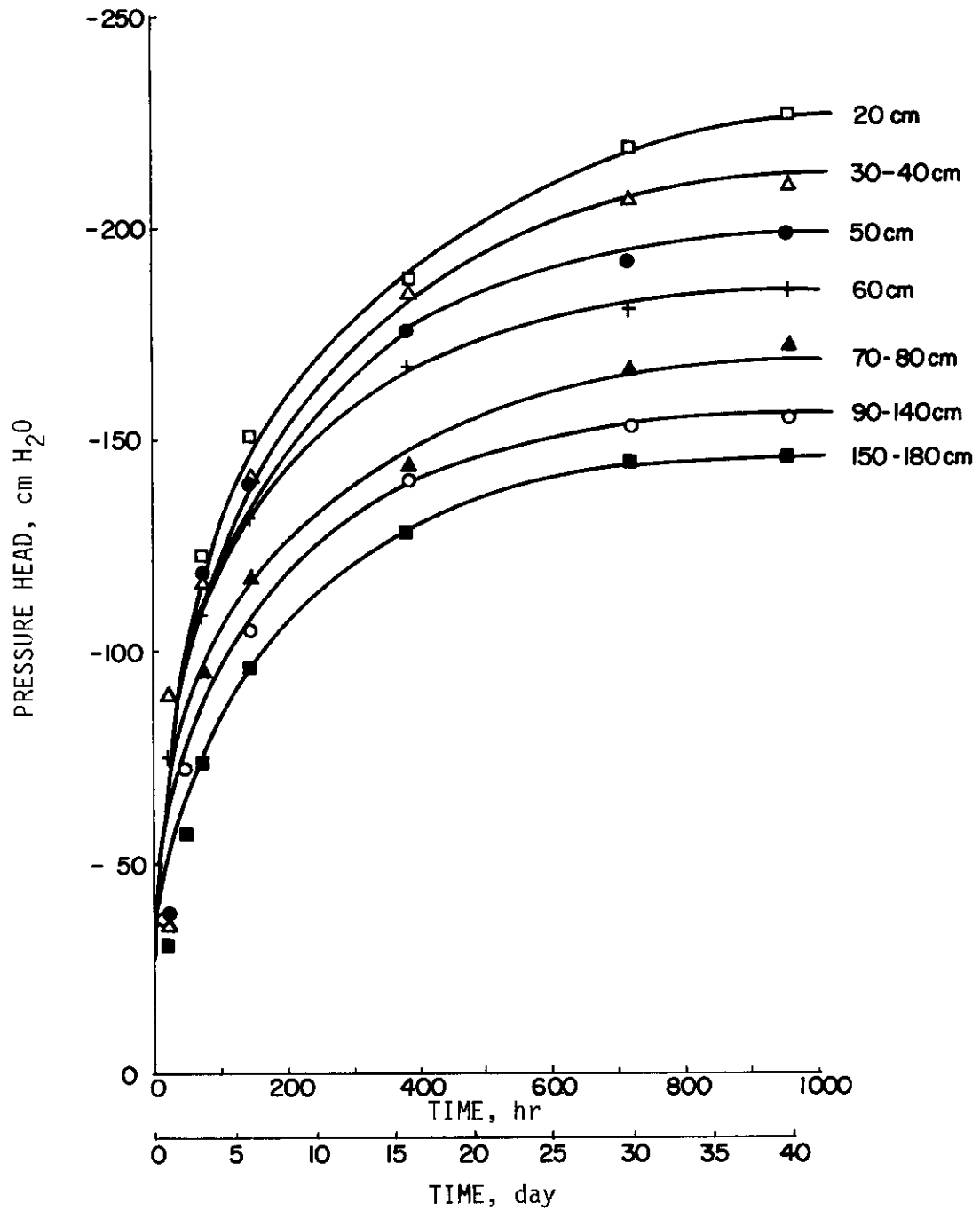


Fig. 8. Tensiometry showing pressure head versus drainage period for each depth. (smoothed data)

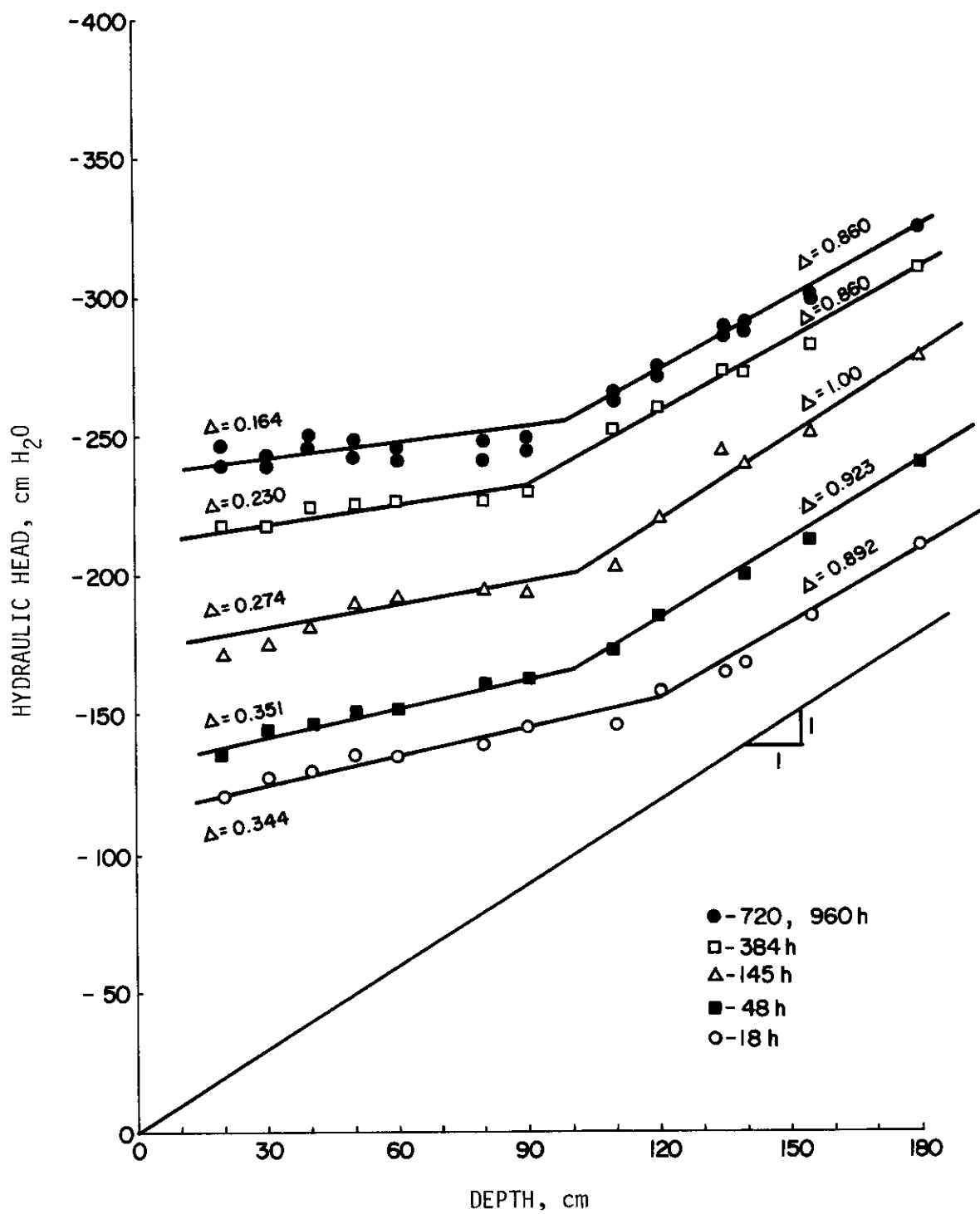


Fig. 9. Hydraulic head profiles for different times. (smoothed data)



less than 0.4 from 0 to 90 cm, but increased sharply to values near unity for depths greater than 90 cm.

The soil water content data are shown in Fig. 10 (p. 36) as volumetric water content versus depth for various times since saturation. The 6-hour data show the maximum water contents; thus, it was used as the initial soil water content curve. The change in water content with time at depths below 90 cm was minimal when compared to the change in soil water content which occurred above this depth. This fact plus the fact that values of  $dH/dz$  were near unity for depths greater than 90 cm (refer to Fig. 9, p. 34) indicated that approximate steady-state flow conditions prevailed in the lower soil layers.

To demonstrate the drainage process, the soil moisture content in each soil layer is plotted versus time in Fig. 11 (p. 37). The rate of change in water content as a function of time was determined from this figure. The volume flux or the total water content change per unit time, through each soil layer, is shown in Fig. 12 (p. 38). Volume flux through each depth increment was obtained by integrating the soil moisture versus time curve (Fig. 11) with respect to depth.

The volume fluxes for the lower soil depths varied only slightly from each other. However, the volume flux in the upper soil layer (30 cm) was less than the volume flux obtained at the other soil

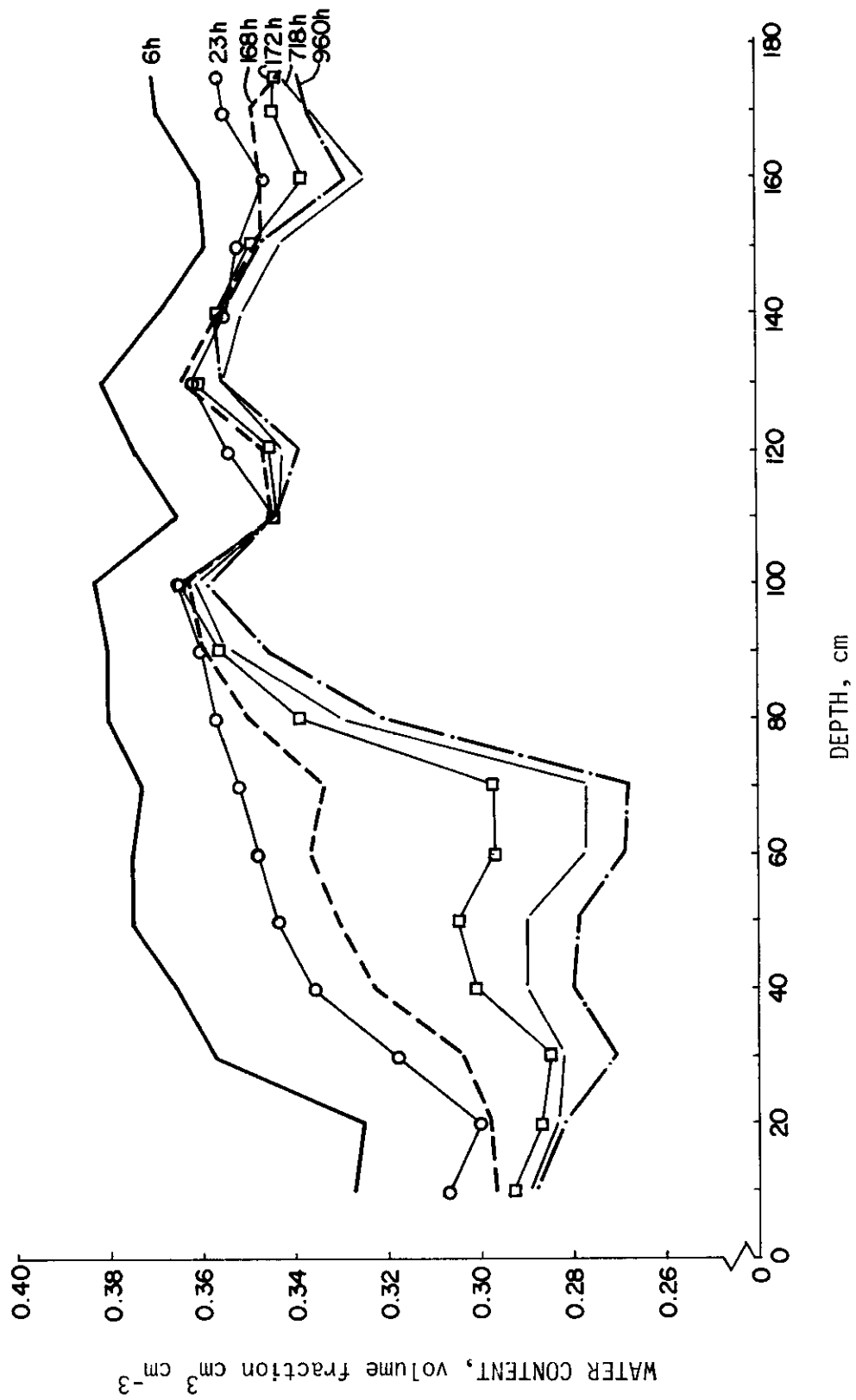


Fig. 10. Soil moisture profiles for different times.

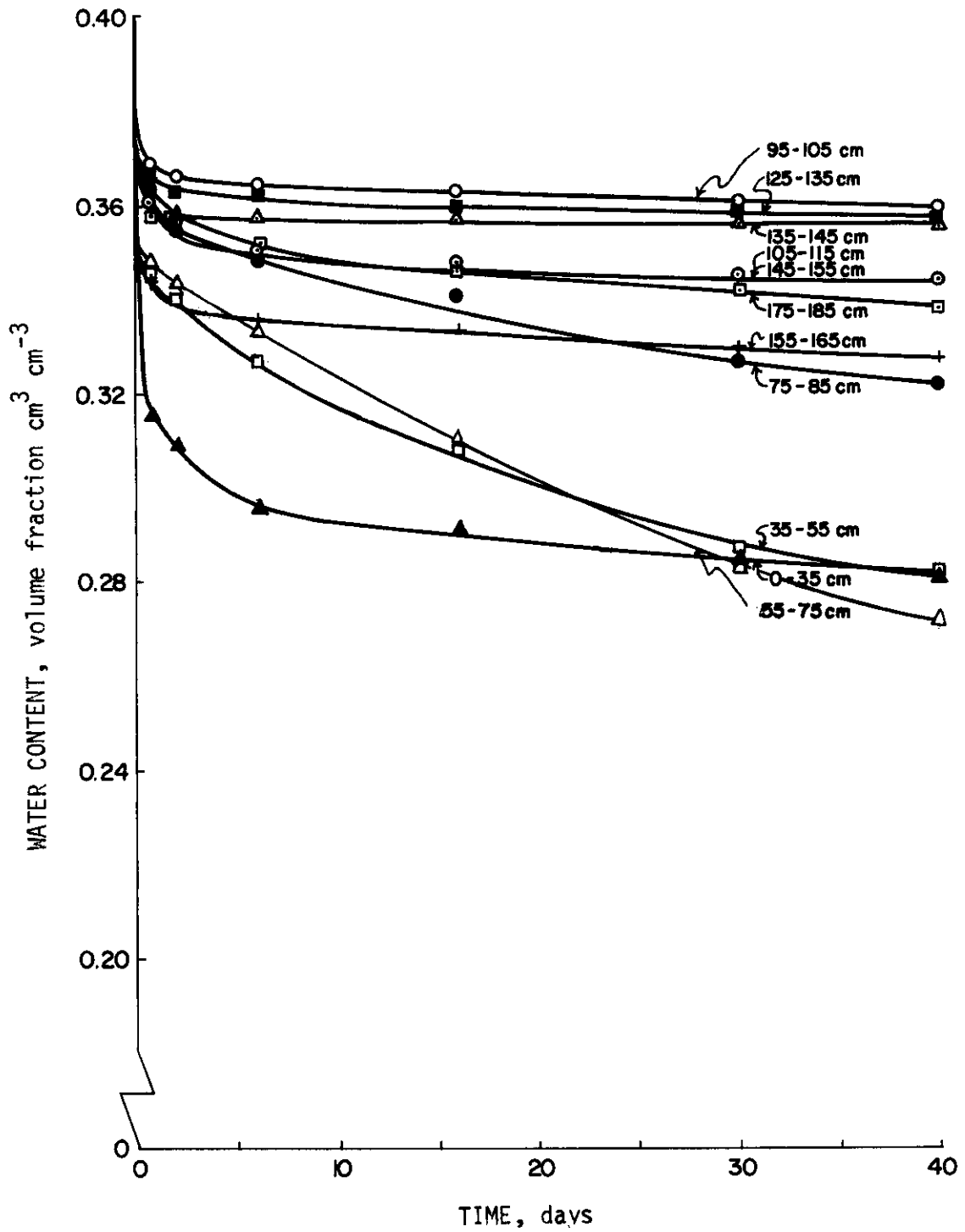


Fig. 11. Soil moisture for different depths.

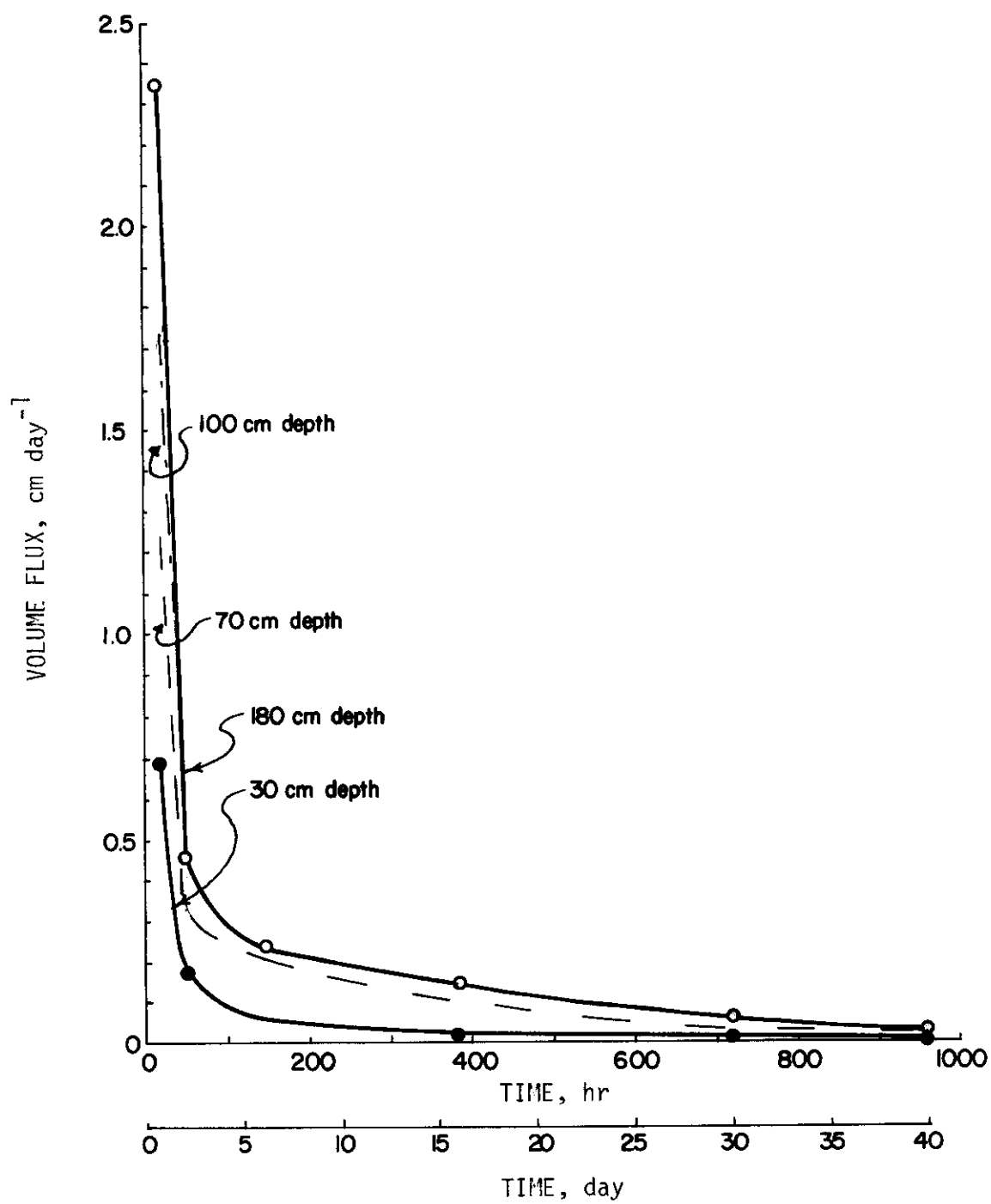


Fig. 12. Volume flux versus time for various depths.

depths. The drainage process for the deeper soil layers continued over a much longer period of time than for the shallow soil depths.

Hydraulic conductivity was calculated at known times and water contents by dividing the volume flux,  $q$ , by the change in hydraulic head,  $dH/dz$  (see Fig. 9, p. 34). It was evident that the relationship between hydraulic conductivity and water content varied with soil depth. Curves for each soil depth are shown in Figs. 13-17 (pp. 40, 41, 42, 43, 44, respectively) and calculations are demonstrated in Appendix A (pp. 75-80). The large slopes ( $dH/dz$ ) for depths below 80 cm would cause considerable error in estimating fluxes with measured gradients for even a small change in water content.

#### Double-tube method.

Saturated hydraulic conductivity was determined for three depths: 10, 40 and 70 cm. Several runs with the double-tube apparatus were necessary before a successful run was executed. Difficulties stemmed from inserting the inner tube into the soil too shallow and poor cleaning of the hole surface. These factors are not recognized until both tubes are in the ground and preliminary data are collected.

The final runs at the three soil depths worked well, however. The data used to calculate the saturated conductivities are presented in Table A-7 and Figs. A-1, A-2 and A-3 of Appendix A. Table 2 (p. 45) shows the outcome of the test and Fig. 18 (p. 46) shows the saturated conductivities versus depth.

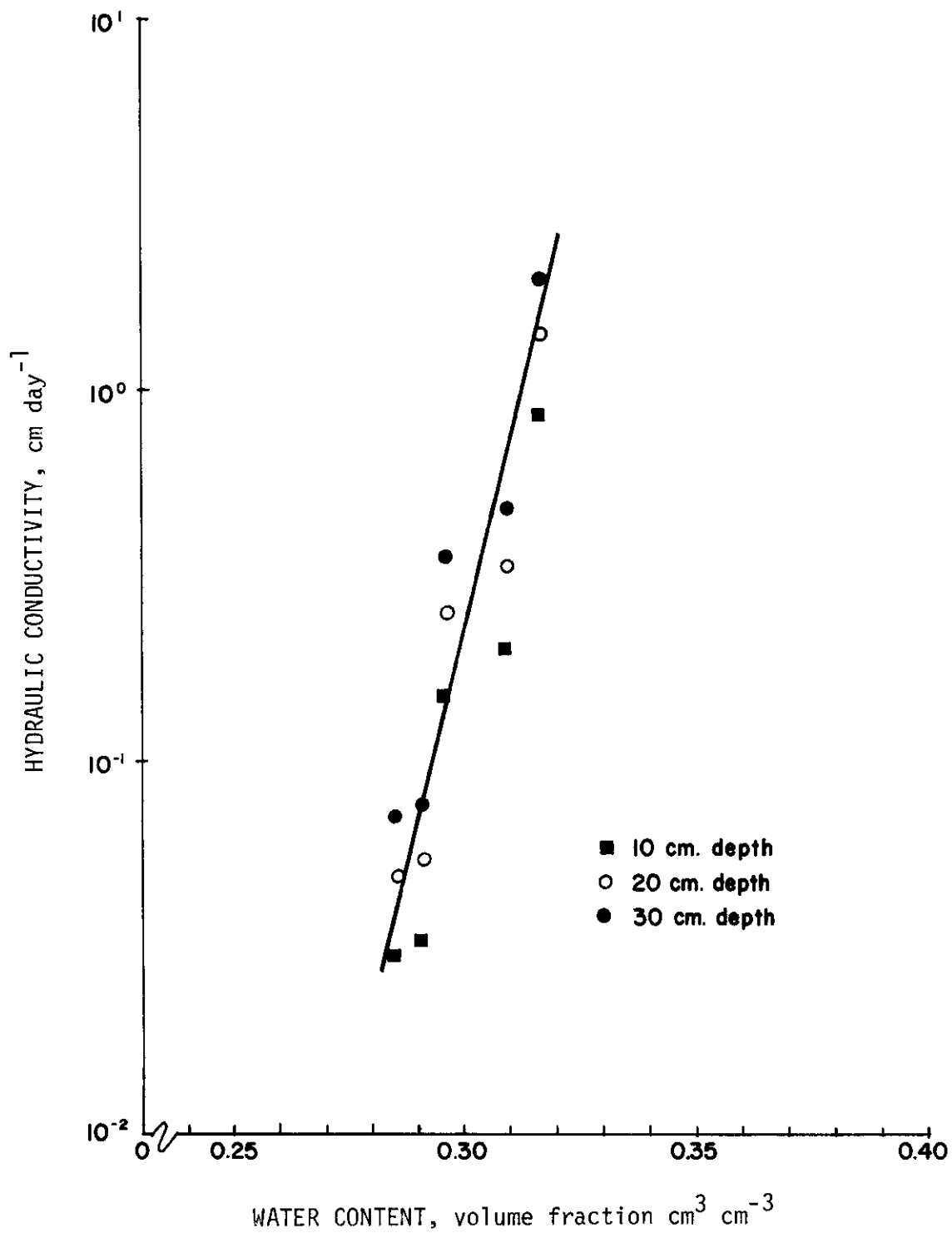


Fig. 13. Relationship between hydraulic conductivity and water content determined from field measurements for 10-30 cm soil depth.

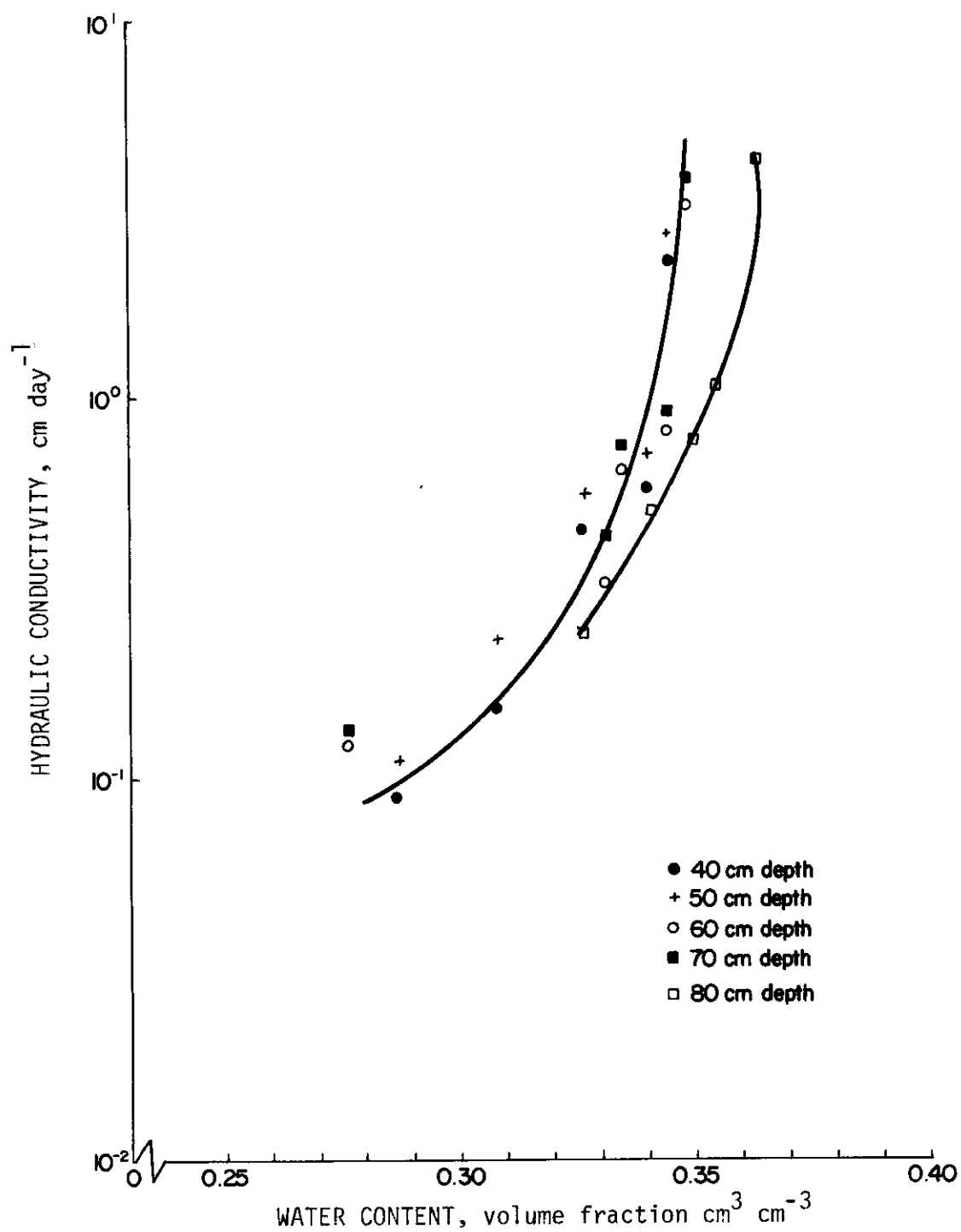


Fig. 14. Relationship between hydraulic conductivity and water content determined from field measurements for 40-80 cm soil depth.

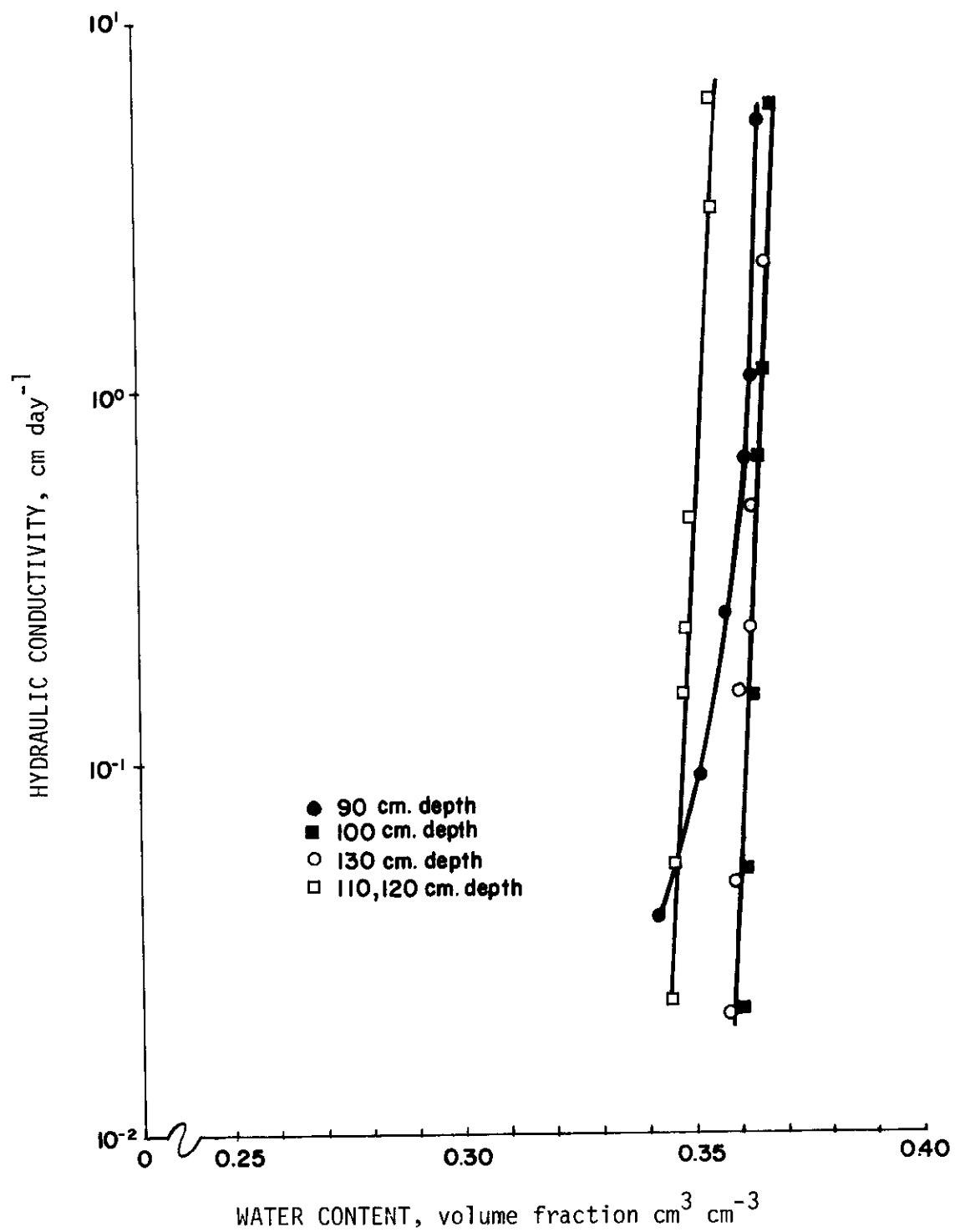


Fig. 15. Relationship between hydraulic conductivity and water content determined from field measurements for 90-120 cm soil depth.



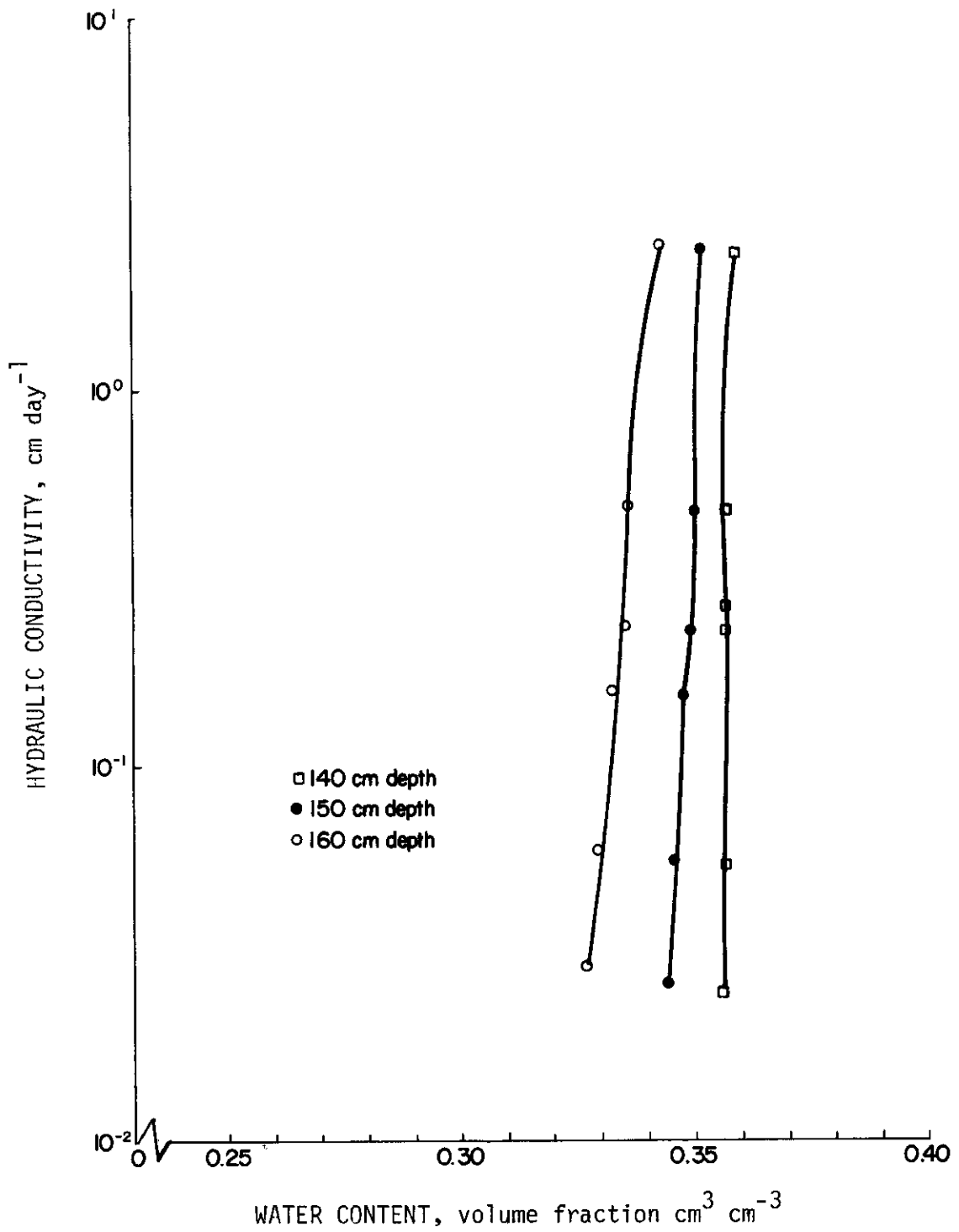


Fig. 16. Relationship between hydraulic conductivity and water content determined from field measurements for 140-160 cm soil depth.

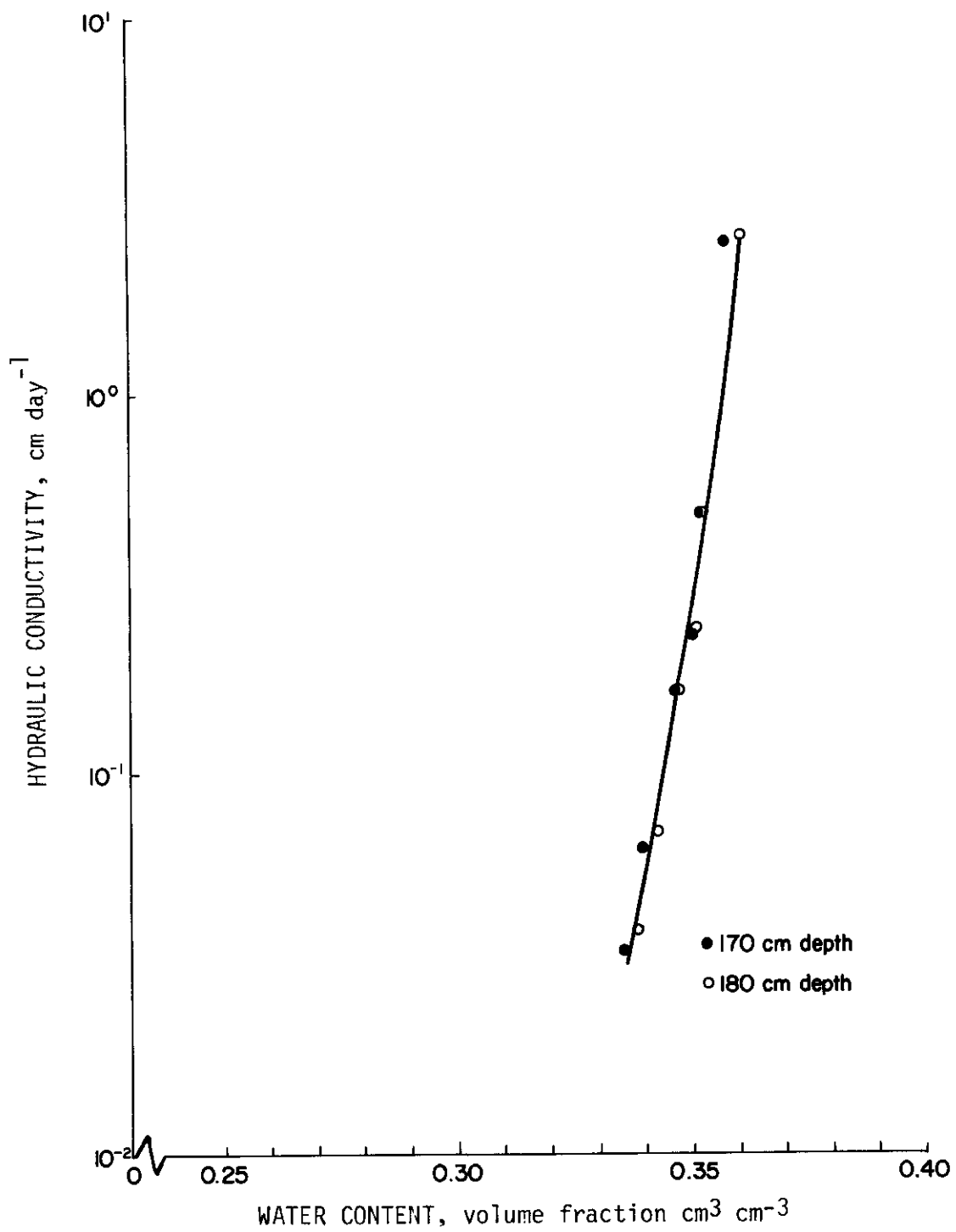


Fig. 17. Relationship between hydraulic conductivity and water content determined from field measurements for 170-180 cm soil depth.

TABLE 2

Saturated Conductivities Measured with Double-Tube Apparatus

<u>Depth, cm</u>	<u>Ks, cm/day</u>	<u>Ks, m/s</u>
10	4.25	$4.9 \times 10^{-7}$
40	40.90	$4.7 \times 10^{-6}$
70	53.44	$6.2 \times 10^{-6}$

SATURATED CONDUCTIVITY  
(measured with double-tube apparatus)

Depth (cm)	Ks (cm/day)	Ks (m/s)
10	4.2	$4.91 \times 10^{-7}$
30	20.9	$2.42 \times 10^{-6}$
40	48.2	$5.58 \times 10^{-6}$
50	60.9	$7.05 \times 10^{-6}$
70	64.8	$7.50 \times 10^{-6}$

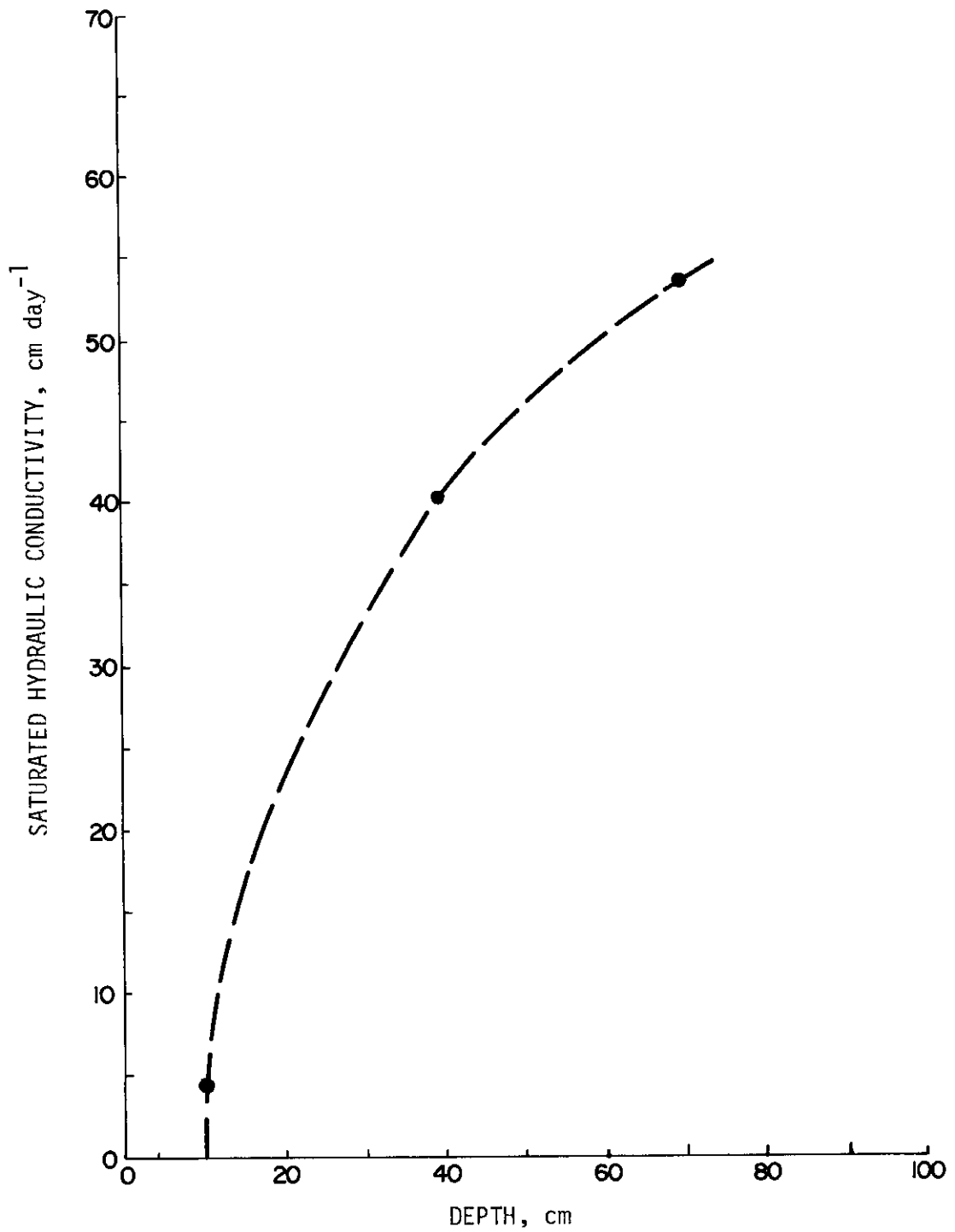
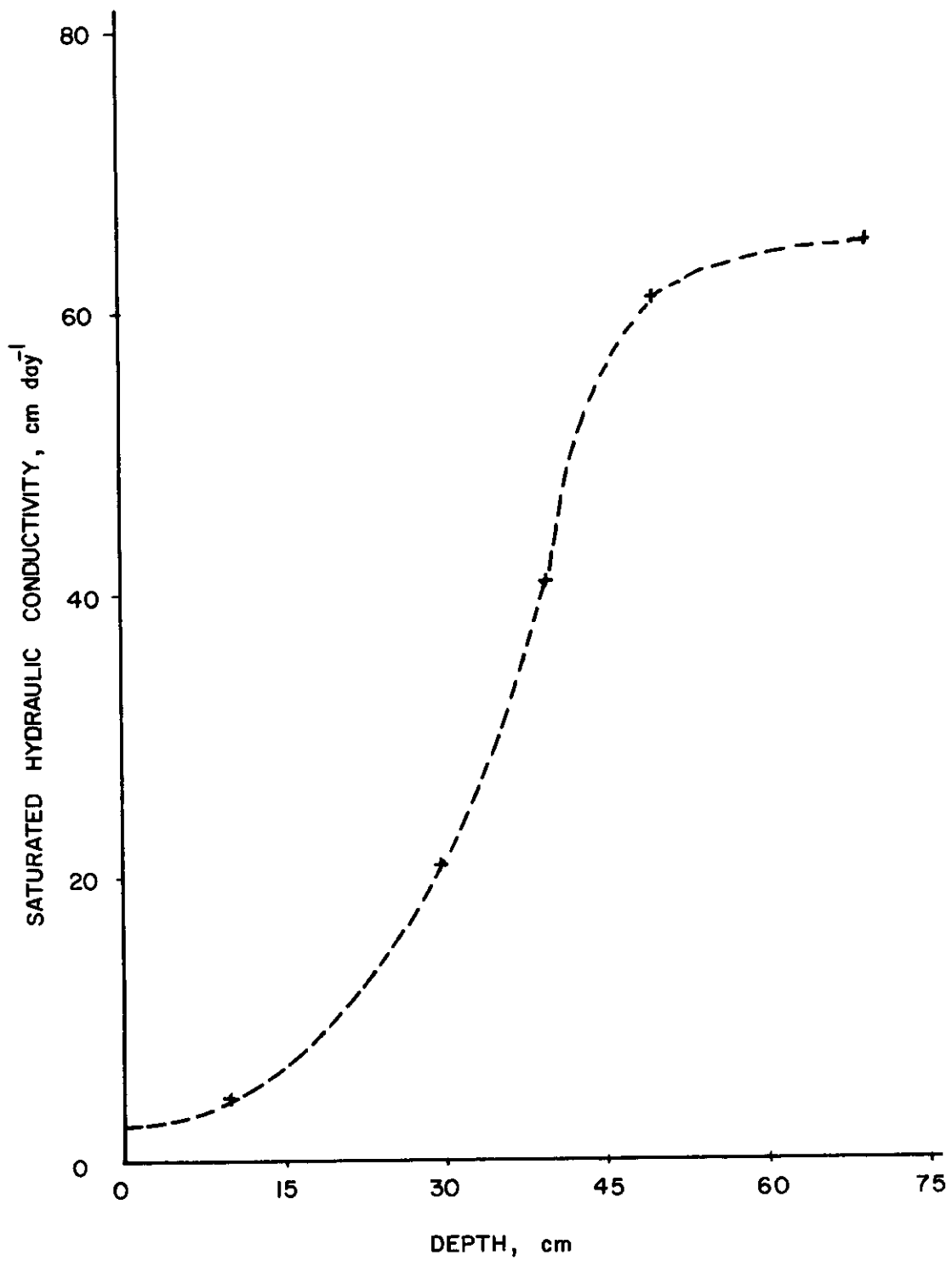


Fig. 18. Saturated hydraulic conductivity versus depth.



Saturated hydraulic conductivity from double-tube method.

### Laboratory Measurements

Water retentivity curves were determined using the pressure-plate extractor data. Soil samples from 0-15, 15-55 and 55-90 cm depth increments were used. However, results for the latter two soil depths were very similar, as can be seen in Figs. 19-21 (pp. 48, 49, and 50, respectively). The values of saturated water contents shown in these figures were theoretically calculated from:

$$S = \frac{100 (p - D_b)}{p} \quad (14)$$

where  $S$  is the total porosity (%),  $p$  is the particle density ( $M/L^3$ ), and  $D_b$  is the bulk density ( $M/L^3$ ). A value of  $2.65 \text{ g/cm}^3$  was used for  $p$ .

Calculations of hydraulic conductivity were made using the relationship in Jackson's procedure. The solid lines in Fig. 22 (p. 51) are the calculated values for the soil depth from 0 to 25 cm using the retentivity curve in Fig. 19 and various saturated hydraulic conductivity ( $K_s$ ) values.  $K_s = 4.25 \text{ cm/day}$  was the measured saturated hydraulic conductivity in the field at the 10 cm soil depth. The other two,  $K_s = 20 \text{ cm/day}$  and  $K_s = 30 \text{ cm/day}$  were roughly estimated from the curve of saturated conductivity versus depth (Fig. 18, p. 46) for the 20 to 25 cm soil depth. The solid dots are the measured values of hydraulic conductivity from the instantaneous profile method for the 0 to 25 cm soil depth. The correlation of calculated (Jackson) to

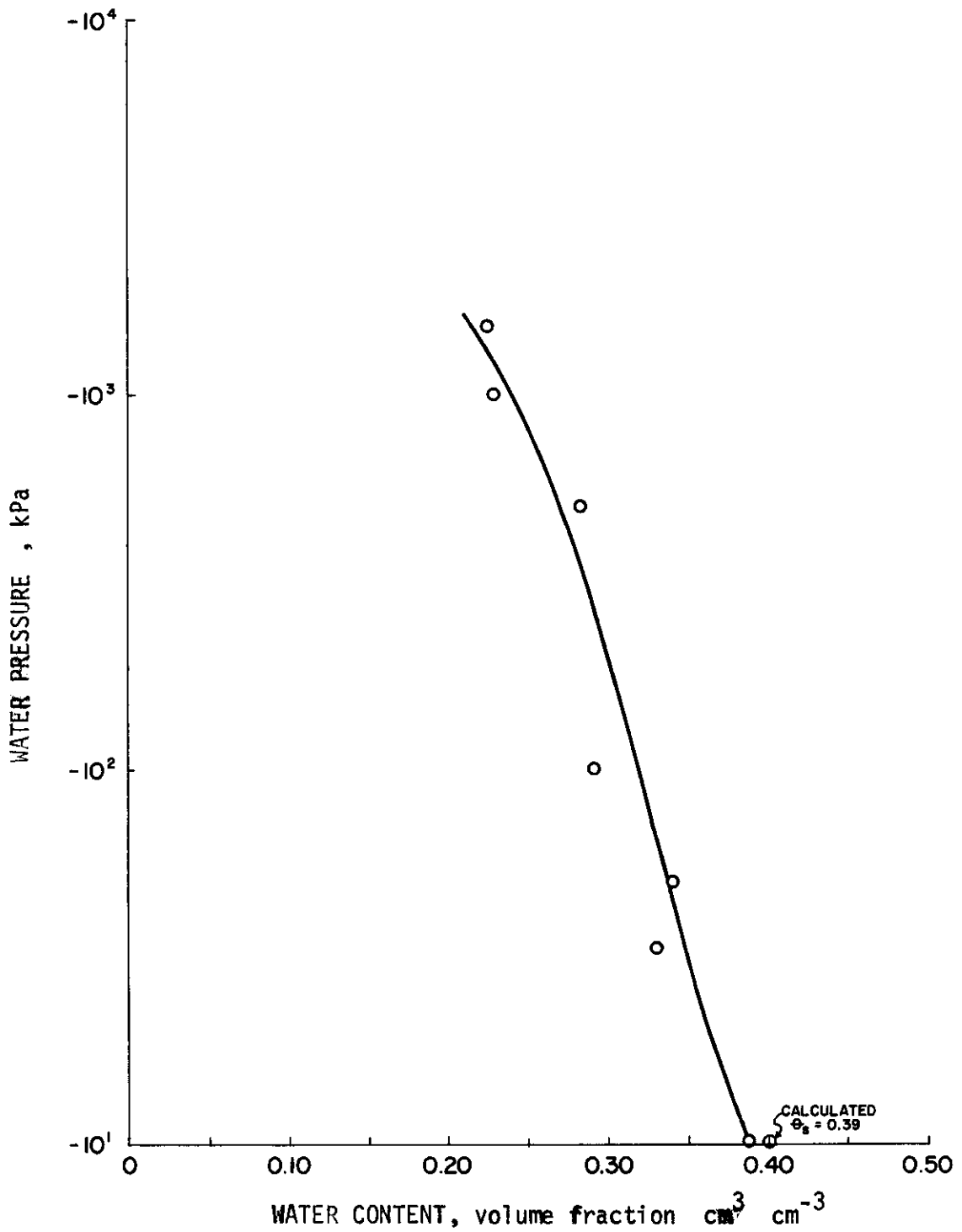


Fig. 19. Water retentivity determined in the laboratory, 0-15 cm soil depth.



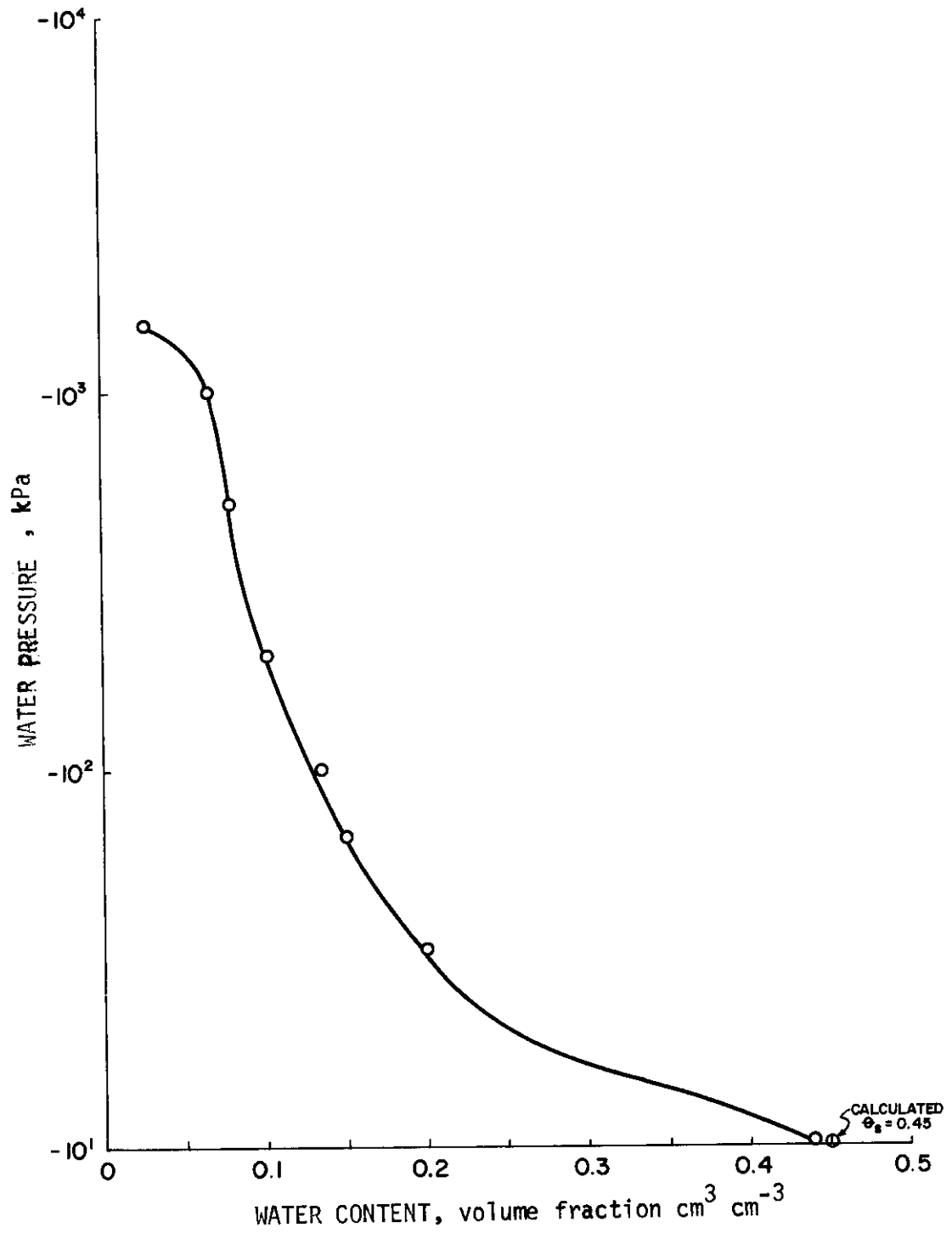


Fig. 20. Water retentivity determined in the laboratory, 15-55 cm soil depth.

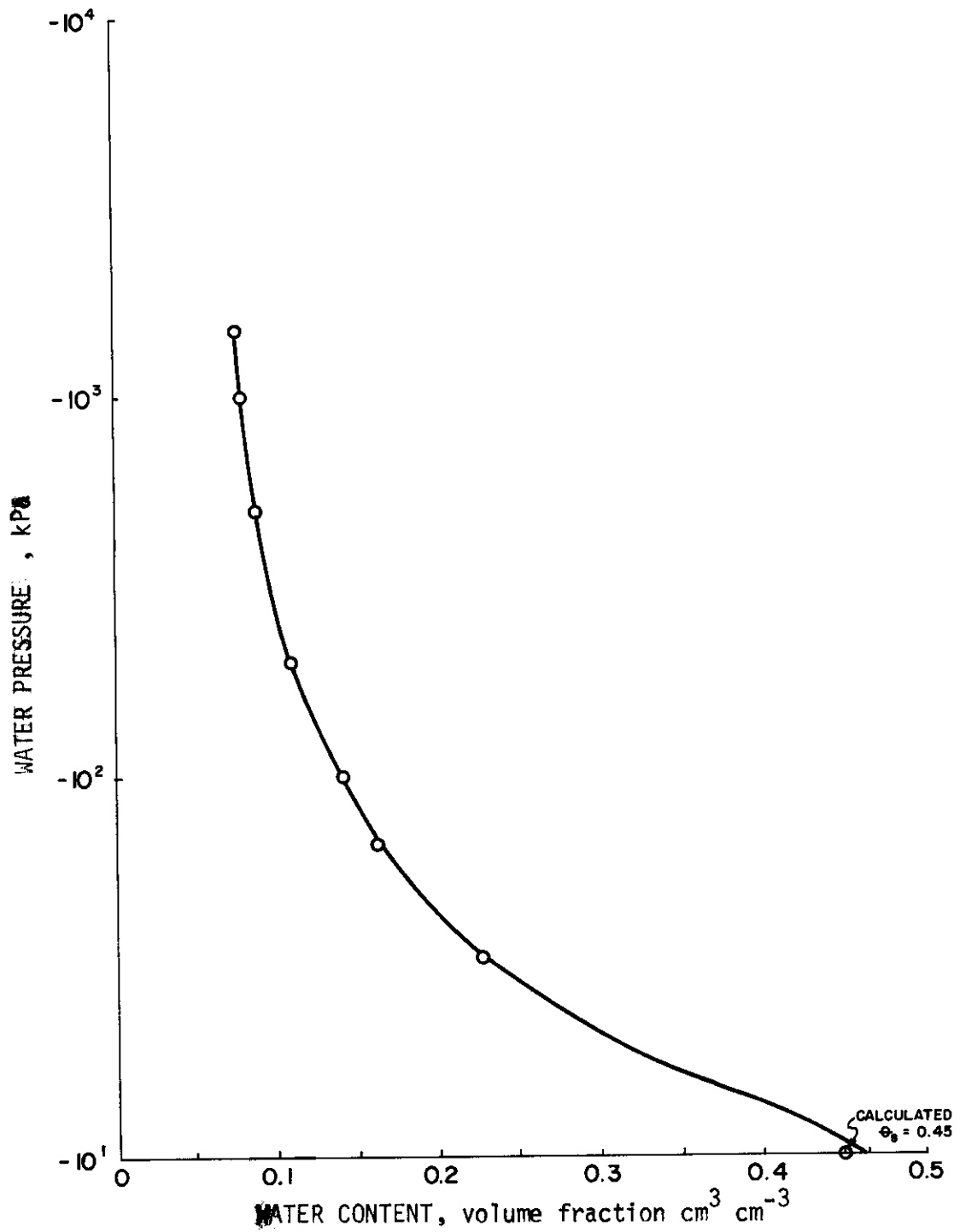


Fig. 21. Water retentivity determined in the laboratory, 55-90 cm soil depth.

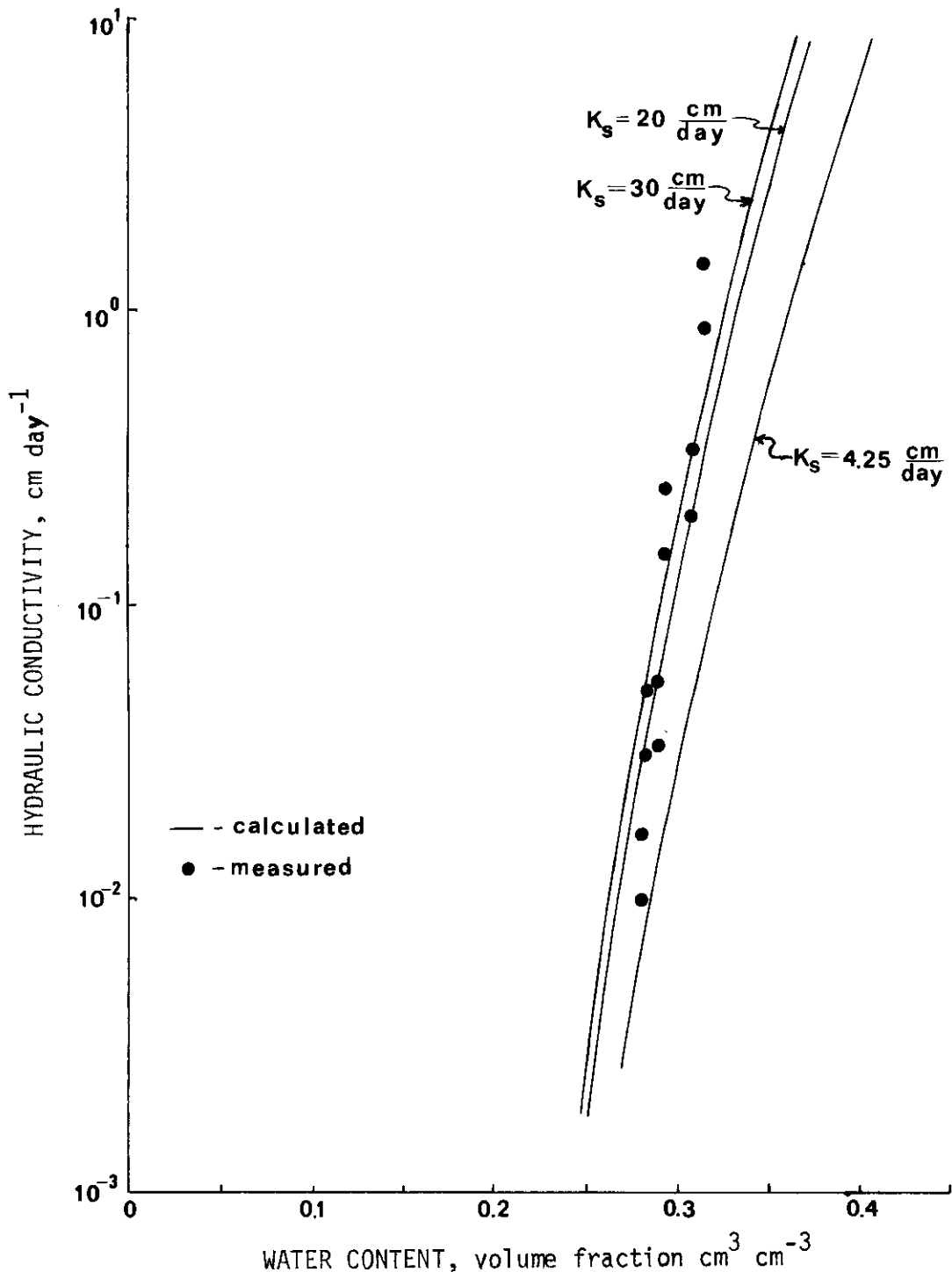


Fig. 22. Comparison of calculated to measured hydraulic conductivity, 0-25 cm soil depth.

to measured (instantaneous profile) is quite good for the 0 to 25 cm depth, particularly for the higher saturated hydraulic conductivity values.

Fig. 23 (p. 53) shows the same comparison, Jackson's procedure for calculation (solid line) and in situ measured values (solid dots) of hydraulic conductivity, for 15 to 55 cm and 55 to 90 cm soil depths. The values of hydraulic conductivity for the 15 to 55 cm depth were calculated from the respective water retention curve (Fig. 20, p. 49) and using  $K_s = 40.9$  cm/day (measured at 40 cm soil depth). The hydraulic conductivity for the second soil depth, 55 to 90 cm, was calculated from the respective water retention curve (Fig. 21, p.50) and with  $K_s = 53.4$  cm/day (measured at 70 cm soil depth). The solid dots are measured hydraulic conductivity for the 30 to 80 cm soil depth. The correlation observed in this comparison was not very good.

Another approach for evaluating the theoretical method for calculating hydraulic conductivity was to use field pressure potential in conjunction with the laboratory retention curves. Because of the limited water content range occurring during the field experiment the field data fell within the higher pressure region so that the laboratory data was used to extrapolate the curves into the lower pressure range as shown in Figs. 24 and 25 (pp. 54 and 55). When these combined retention curves were used with Jackson's procedure, little difference

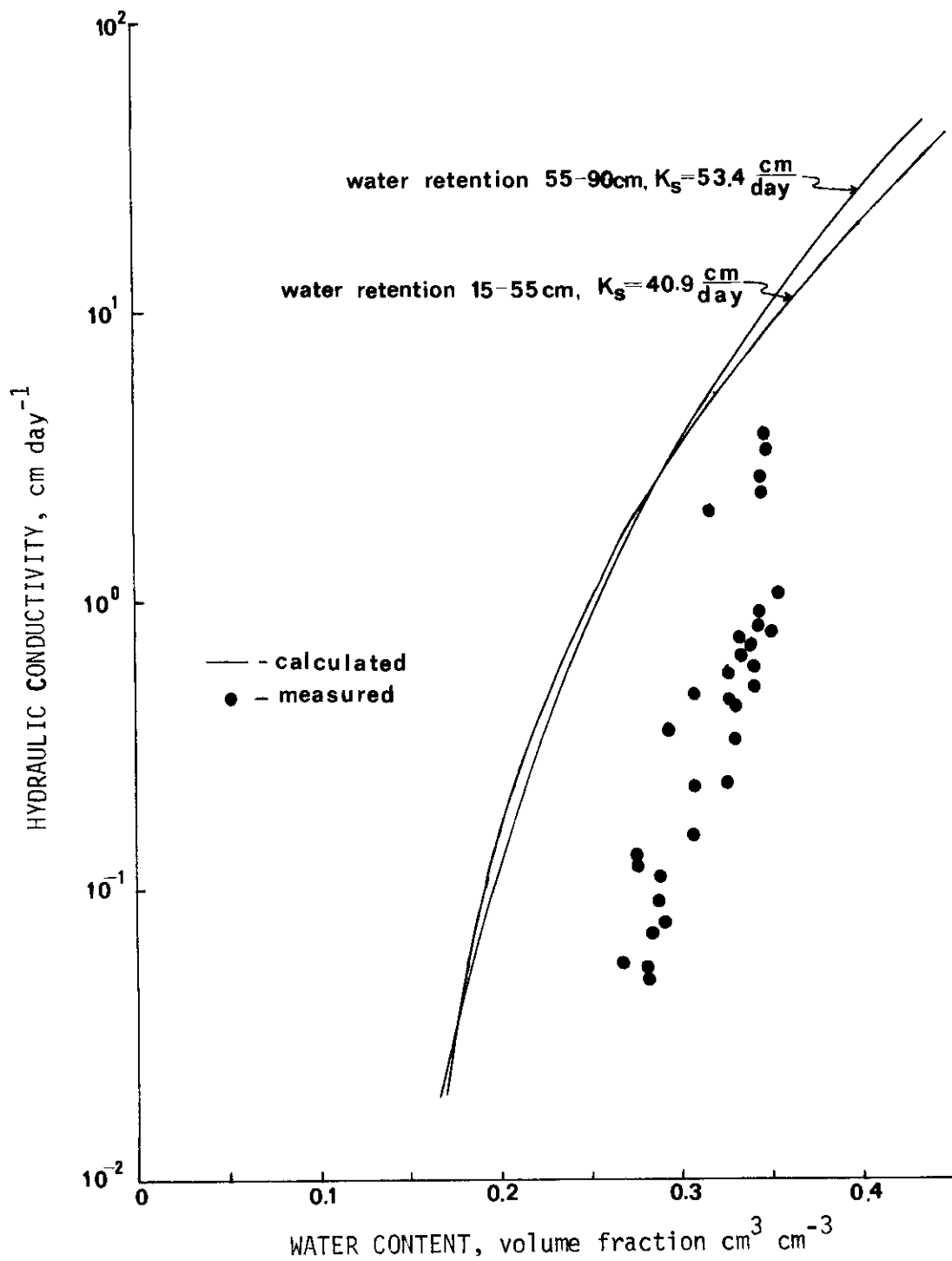


Fig. 23. Comparison of calculated to measured hydraulic conductivity, 30-80 cm soil depth.

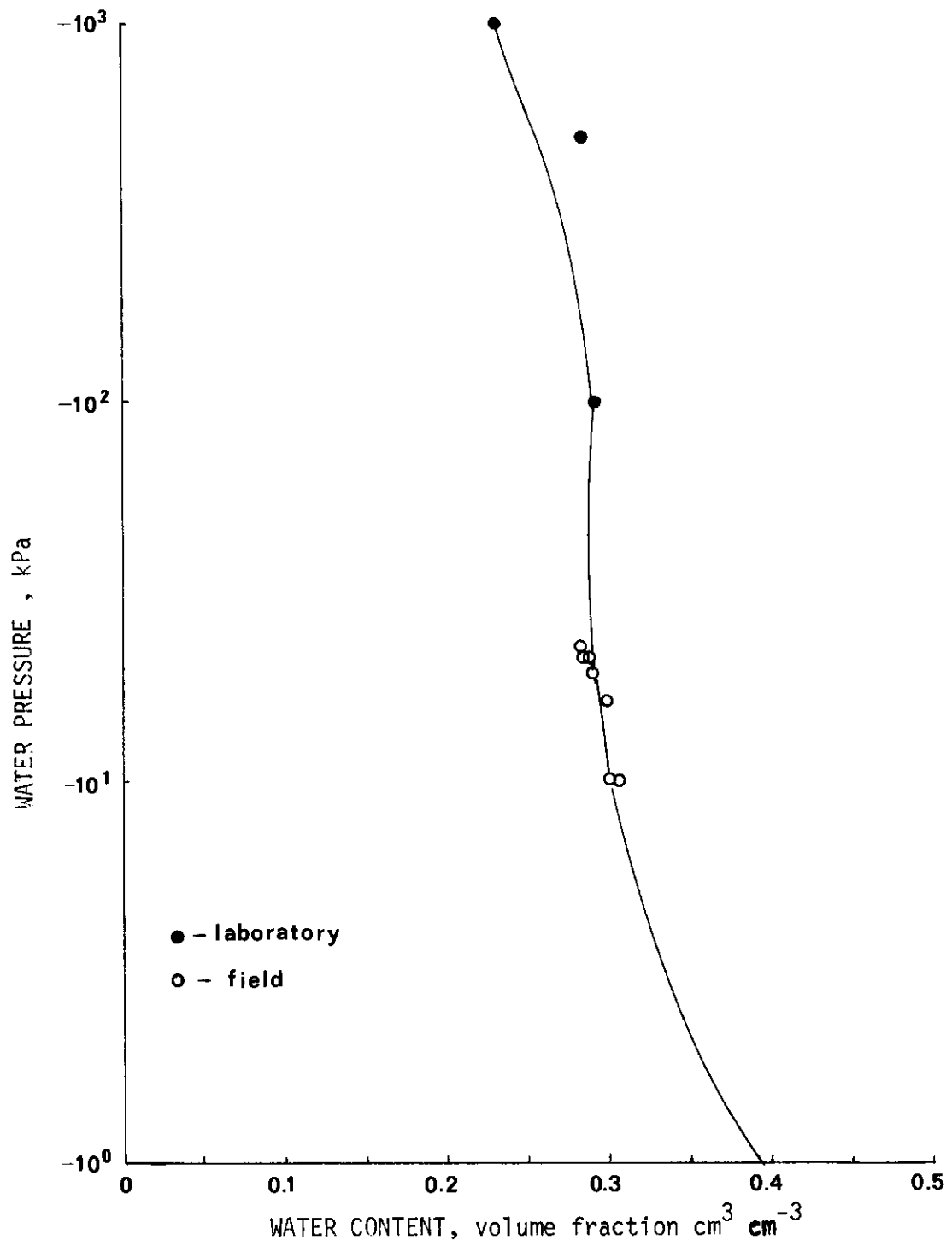


Fig. 24. Water retentivity from field data combined with laboratory data, 0-25 cm soil depth.

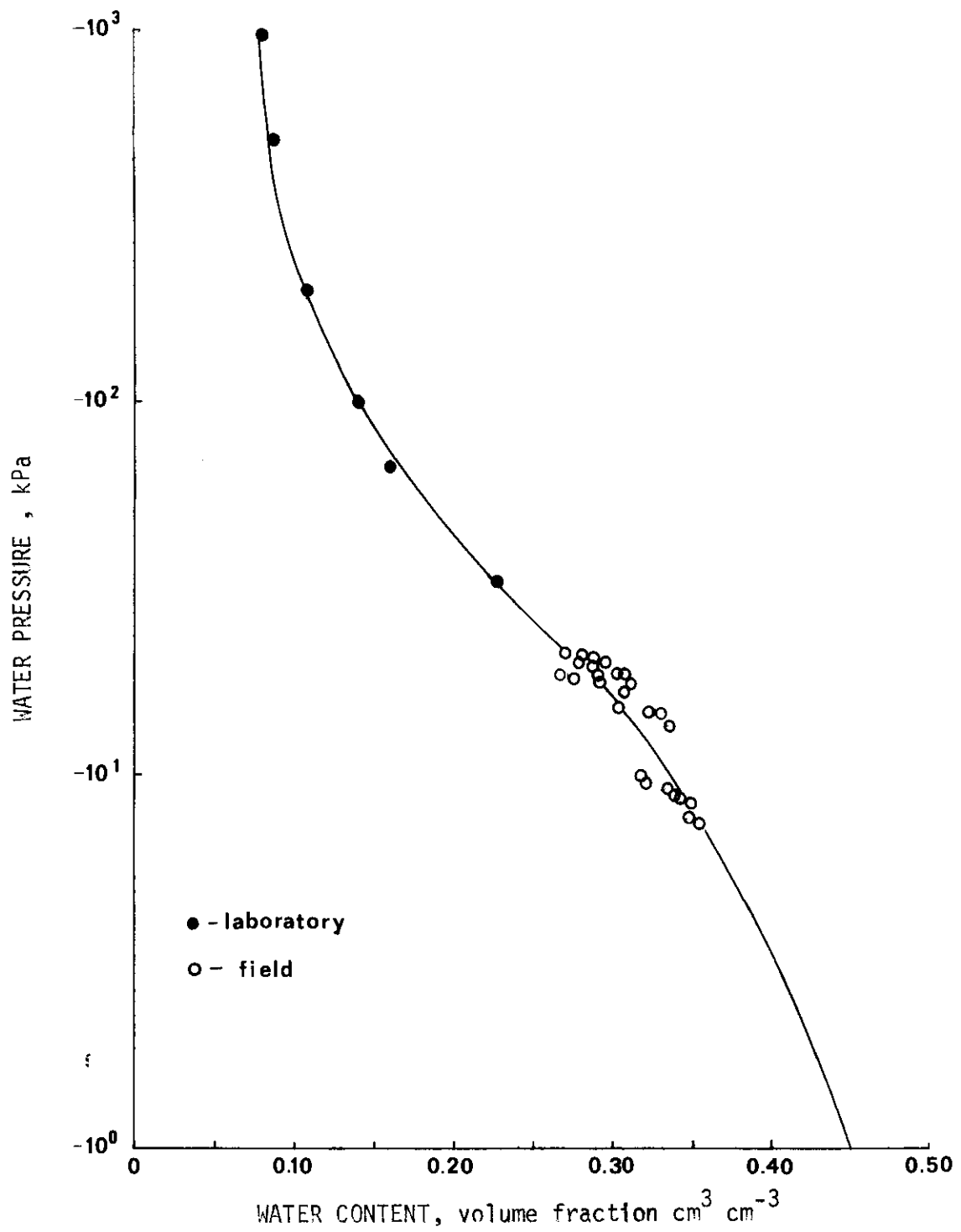


Fig. 25. Water retentivity from field data combined with laboratory data, 15-55 cm soil depth.

was observed for the 0 to 25 cm soil depth (Fig. 26, p. 57) but a better correlation was obtained between the field and calculated values of hydraulic conductivity for the 30 to 80 cm soil depth range (Fig. 27, p. 58).

The method used to obtain soil samples for measuring water retention in the laboratory was the major cause for these discrepancies between measured and calculated values of hydraulic conductivity. The difference between using the laboratory only and the combined laboratory and field retentivity curves was small at the 0 to 15 cm soil depth yet the difference between the two approaches was much greater at the deeper soil depths. The 0 to 15 cm soil depth was sampled with a volumetric soil sampler, and the entire soil core was used in the test; whereas, the deeper soil depths were sampled using a soil auger and the soil used in the test was loose. It was concluded that Jackson's method of calculating soil hydraulic conductivity versus water content is relatively accurate provided the input data from the water retentivity curves are representative.

#### Centrifuge Method

The technique was set up to utilize readily available laboratory equipment. Difficulties were encountered with the weighing method. The soil cores weighed approximately 400 g and an analytical balance to accurately weigh above 200 g in milligrams was not available.





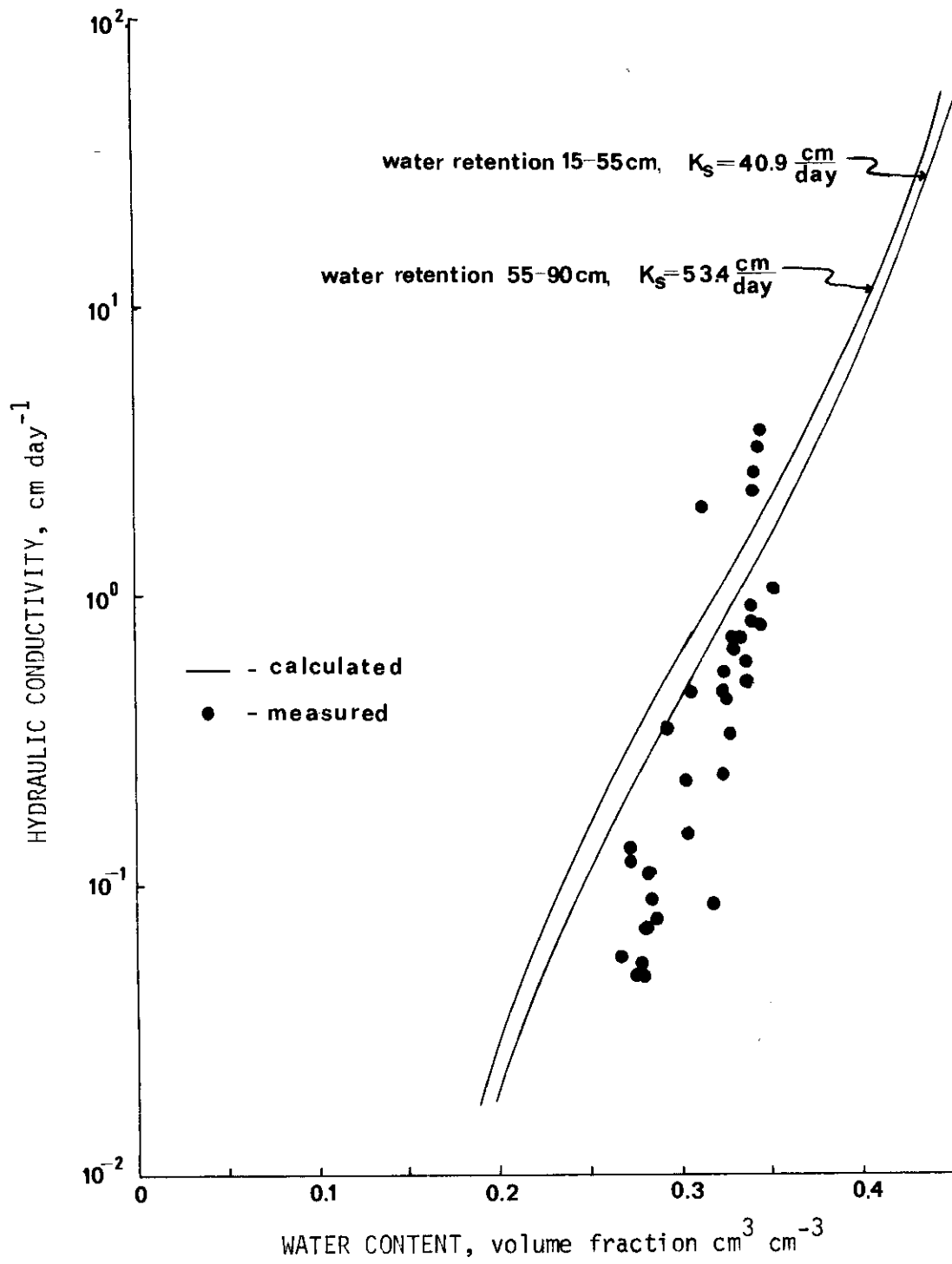


Fig. 27. Comparison of calculated to measured hydraulic conductivity, 30-80 cm soil depth.

Therefore, a balance with an accuracy in centigrams was used and estimation of milligrams was made.

Most of the measurements obtained with the centrifuge method were clearly erroneous. When measurements were plotted to match the theoretical curve for diffusivity, there was no possible correlation. Certain runs, however, yielded data consistent with the theoretical equation. The discrepancies were attributed in part to drafts and air movement within the room which interfered with readings on the analytical balance and reduced the desired accuracy. As a matter of interest, values of hydraulic conductivity obtained from these data are presented in Figs. 28, 29 and 30 (pp. 60, 61 and 62). Definite conclusions could not be made as to the applicability of the centrifuge method in this study.

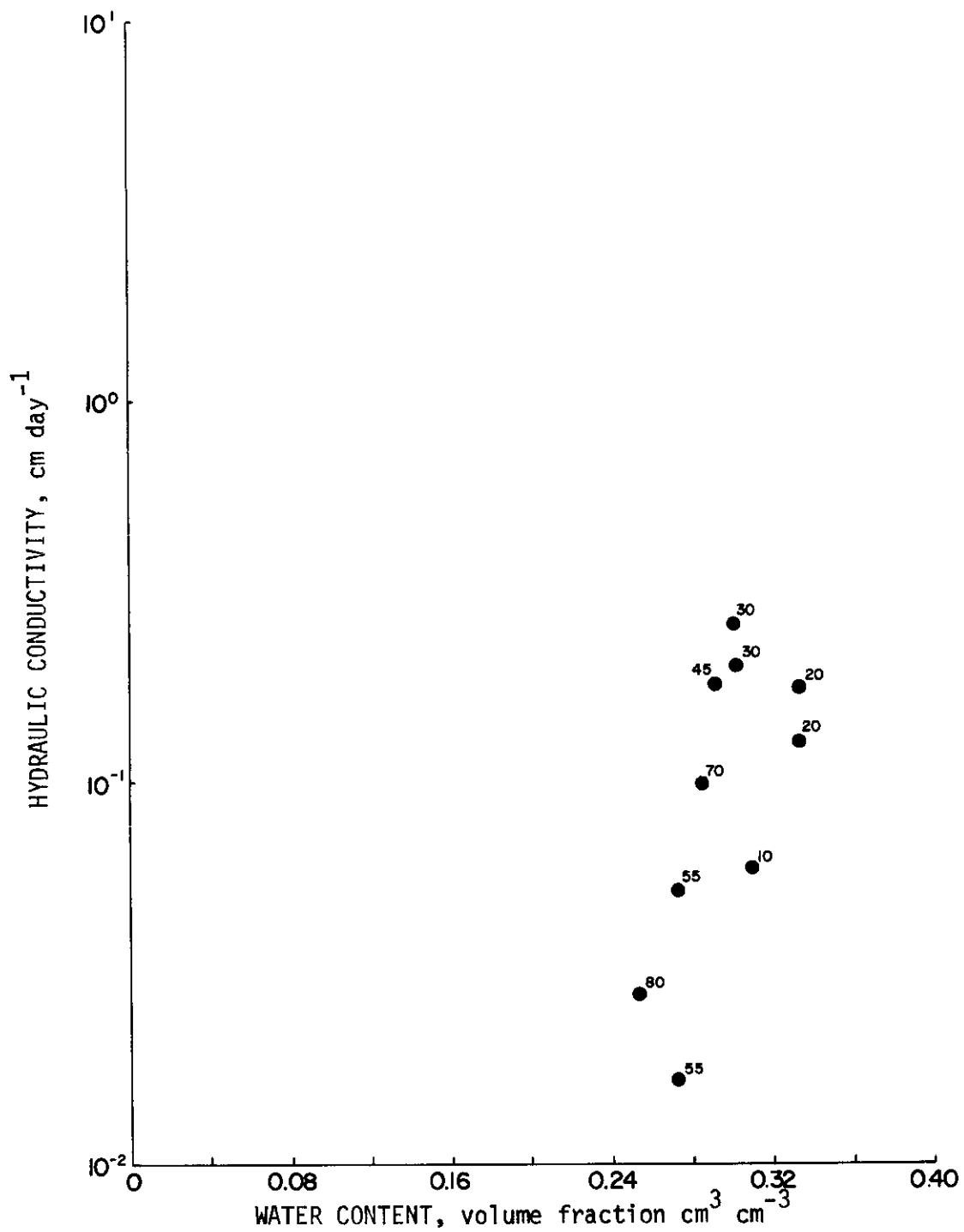


Fig. 28. Hydraulic conductivity versus water content determined from centrifuge data for noted soil depths.

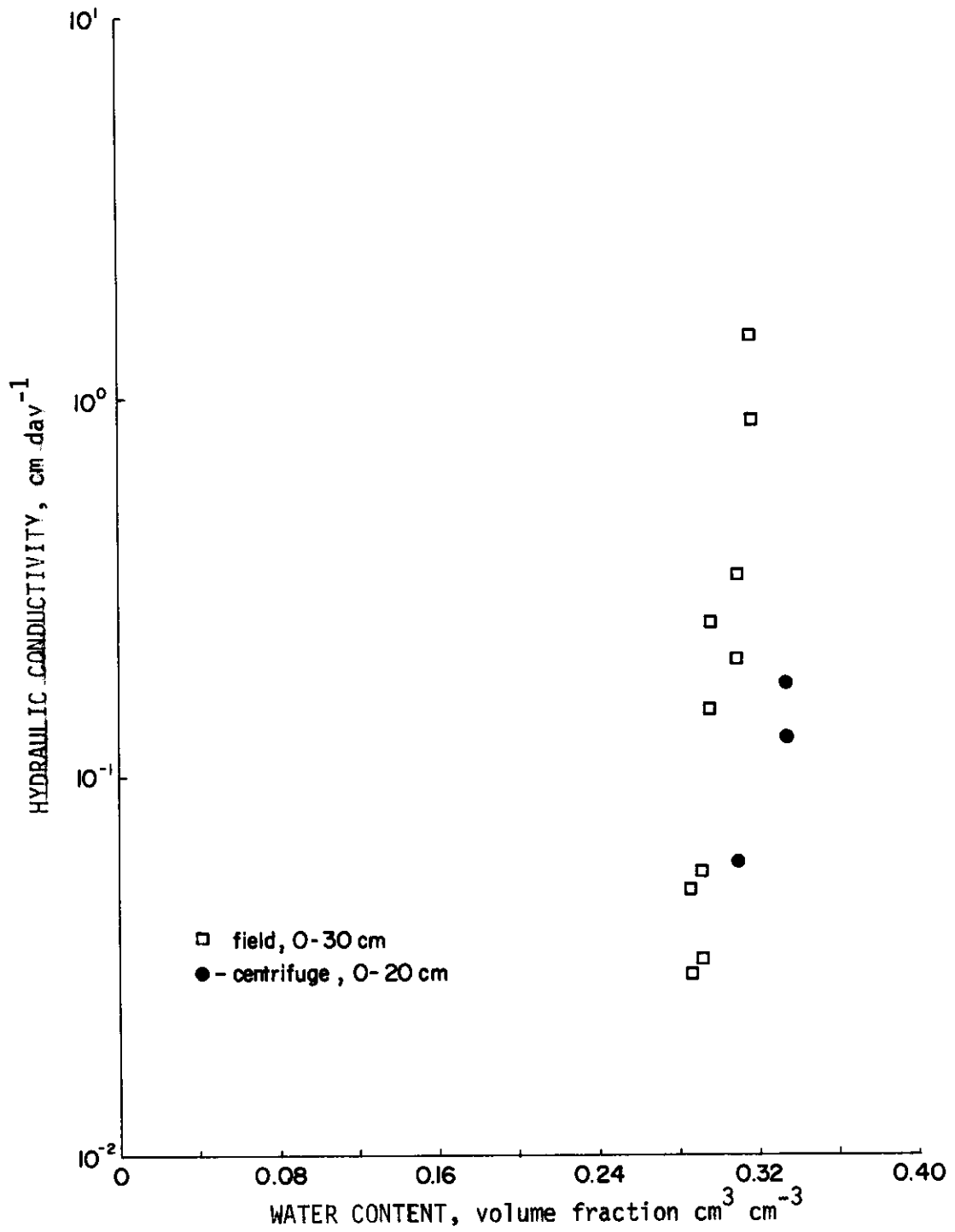


Fig. 29. Comparison of laboratory to field hydraulic conductivity, 0-30 cm soil depth.

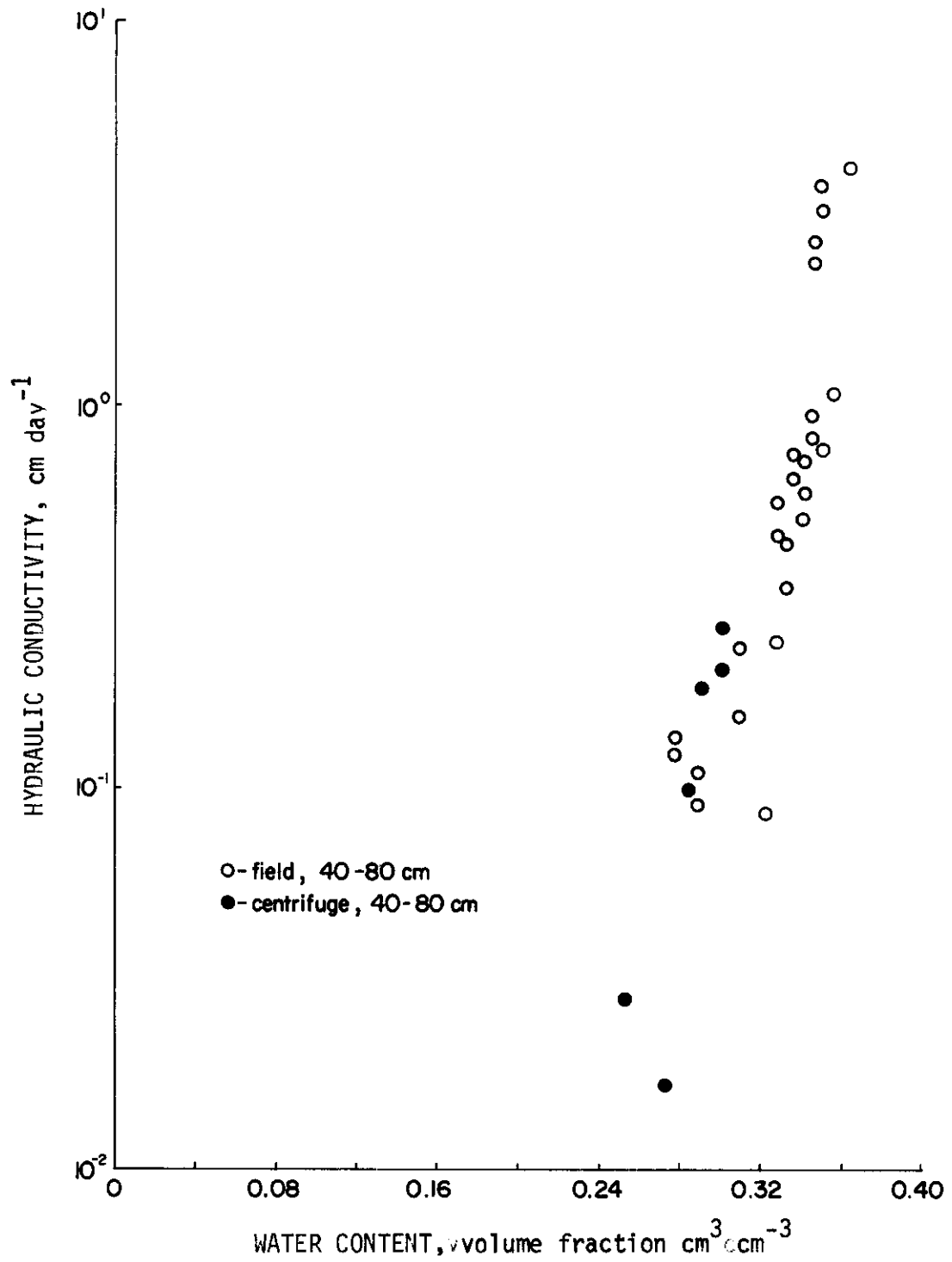


Fig. 30. Comparison of laboratory to field hydraulic conductivity, 40-80 cm soil depth.



## CHAPTER V

### SUMMARY AND CONCLUSIONS

Laboratory or mathematical techniques for determining soil hydraulic properties are more practical than field experiments provided they yield accurate results. The purpose of this study was to evaluate a theoretical technique and a laboratory method of determining hydraulic conductivity by comparison with results measured in situ.

The soil was of the Norwood Series, Typic Udifluent. A field plot was monitored for water content and pressure head during drainage from saturation with evaporation prevented. Measurements were obtained with a neutron moisture probe and tensiometers. The resulting data from the soil profile provided the necessary information for calculation of hydraulic conductivity.

The soil profile was characterized by several relations of hydraulic conductivity, varying with depth. The reason for this was attributed to the heterogeneous nature of the profile due to variance in clay content. Because of the narrow range of water content over the period of measurement, particularly below a soil depth of 100 cm, the range of hydraulic conductivity values was also limited.

The laboratory method for measuring hydraulic conductivity was centrifugation (Alemi, et al., 1972). Because of difficulties with the



weighing procedure, results were extremely inconsistent and few runs were successful. Conclusive recommendations cannot be made as to the applicability of this method from this study because of limited results.

The theoretical method for predicting hydraulic conductivity utilized water retention curves and saturated hydraulic conductivity values. The pressure-water content curve was obtained with pressure plate extractors using disturbed soil samples. Saturated conductivities were determined for 10, 40 and 70 cm soil depths using Bouwer's (1961) double-tube method.

The theoretical method underpredicted hydraulic conductivities at the soil surface (0 to 15 cm soil depths) and grossly overpredicted hydraulic conductivities in the 30 to 80 cm range of soil depths. When the water retention curves were modified by including data obtained in the field with the laboratory data, the resulting calculations of hydraulic conductivity reasonably predicted field values. This model was sensitive to the pressure versus water content relationship and accuracy in measuring this relationship is necessary.

#### Recommendations for Future Study

It is suggested that for additional studies using the methods described (1) evaluation of the centrifuge method will require a measuring device to accurately detect the movement of water within the

soil core and (2) extensive measurements of water retentivity relations in the laboratory and field are necessary for further comparison and evaluation. Spatial variation of soil properties in the field should be determined and possibly described by statistical methods to aid in determining in situ sample size for further studies of this type.



## REFERENCES

- 1 Alemi, M. H., D. R. Nielsen and J. W. Biggar. 1976. Determining the hydraulic conductivity of soil cores by centrifugation. *Soil Science Society of America Proceedings* 40:212-218.
- 2 Bouwer, Herman. 1961. A double tube method for measuring hydraulic conductivity of soil in situ above a water table. *Soil Science Society of America Proceedings* 25:334-449.
- 3 Bouwer, H. and R. D. Jackson. 1974. Determining soil properties. p. 611-666. In: Jan van Schilfgaarde (ed.). *Drainage for Agriculture. Agronomy Nomograph 17*, American Society of Agronomy, Madison, WI.
- 4 Bruce, R. R. and A. Klute. 1956. The measurement of soil moisture diffusivity. *Soil Science of America Proceedings* 20:458-462.
- 5 Childs, E. C. and N. Collis-George. 1950. The permeability of porous materials. *Proceedings Royal Society* 201A:392-405.
- 6 Day, D. R. 1965. Particle fractionation and particle-size analysis. p. 545-566. In: C. A. Black (ed.). *Methods of soil analysis. Agronomy Nomograph 9*, American Society of Agronomy, Madison, WI.
- 7 Doering, E. J. 1964. Soil water diffusivity by the one step method. *Soil Science* 99:322-326.
- 8 Gardner, W. R. 1956. Calculation of capillary conductivity from pressure plate outflow data. *Soil Science Society of America Proceedings* 20:317-320.
- 9 Green, R. E. and J. C. Corey. 1971. Calculation of hydraulic conductivity: a further evaluation of some predictive methods. *Soil Science Society of America Proceedings* 35:3-8.
- 10 Hillel, D., V. D. Krentos and Y. Sylianou. 1972. Procedures and test of an internal drainage method for methods for measuring soil hydraulic characteristics in situ. *Soil Science* 114:395:400.
- 11 Jackson, R. D. 1972. On the calculation of hydraulic conductivity. *Soil Science of America Proceedings* 36:380-382.

- 12 Jackson, R. D., R. J. Reginato, and C. H. M. van Bavel. 1965. Comparison of measured and calculated hydraulic conductivities of unsaturated soils. *Water Resources Research* 1:375-380.
- 13 Klute, A. 1965a. Laboratory measurement of hydraulic conductivity of unsaturated soil. p. 253-261. In: C. A. Black (ed.). *Methods of soil analysis. Agronomy Nomograph 9*, American Society of Agronomy, Madison, WI.
- 14 Klute, A. 1965b. Soil water diffusivity, p. 262-272. In: C. A. Black (ed.). *Methods of soil analysis. Agronomy Nomograph 9*, American Society of Agronomy, Madison, WI.
- 15 Kunze, R. J., G. Uzghara, and K. Graham. 1968. Factors important in the calculation of hydraulic conductivity. *Soil Science Society of America Proceedings* 32:760-765.
- 16 Marshall, T. J. 1958. A relation between permeability and size distribution of pores. *Journal of Soil Science* 9:1-8.
- 17 Millington, R. J., and Quirk, J. P. 1959. Permeability of porous media. *Nature* 183:387-388.
- 18 Millington, R. J., and Quirk, J. P. 1960. Transport in porous media. *International Congress of Soil Science Transactions 7th*, Madison, WI 1:97-107.
- 19 Richards, L. A. 1931. Capillary conduction of liquids through porous systems. *Journal of Applied Physics* 1:318-333.
- 20 Richards, L. A. 1947. Pressure-membrane apparatus, construction and use. *Agricultural Engineering* 28:451-454, 460.
- 21 Richards, S. J. 1965. Soil suction measurements with tensiometers. p. 153-163. In: C. A. Black (ed.). *Methods of soil analysis. Agronomy Nomograph 9*, American Society of Agronomy, Madison, WI.
- 22 van Bavel, C. H. M., P. R. Nixon and V. L. Hauser. 1963. Soil moisture measurement with the neutron method. ARS-41-70. 39 pp.

- 23 van Bavel, C. H. M., G. B. Stirk and K. J. Brust. 1968. Hydraulic properties of a clay loam soil and the field measurement of water uptake by roots, I, Interpretation of water content and pressure profiles. Soil Science of America Proceedings 32:310-317.
- 24 Watson, K. K. 1966. An instantaneous profile method for determining the hydraulic conductivity of unsaturated porous media. Water Resources Research 2:709-715.

APPENDIX A  
Supplementary Data

TABLE A-1  
Field Measurement of Bulk Density

<u>Depth</u> (cm)	<u>Gamma Probe</u> (g/cm <sup>3</sup> )	<u>Avg. Gravimetric</u> (g/cm <sup>3</sup> )
10	1.570	1.590
	1.562	
20	1.643	1.497
	1.631	
	1.592	
30	1.610	1.439
35		1.458
40	1.470	1.465
	1.560	
50	1.465	1.426
	1.467	
60	1.486	1.505
	1.491	
65		1.520
70	1.550	1.430
	1.491	
75		1.436
80	1.550	
	1.495	
90	1.591	
	1.551	
100	1.610	
	1.605	
110	1.660	
	1.664	
120	1.669	
	1.686	
130	1.674	
	1.653	
140	1.690	
	1.660	
150	1.681	
	1.672	
160	1.665	
	1.643	
170	1.663	



TABLE A-2

## Neutron Probe Calibration Data

Surface, 0-15 cm

Line of Best Fit,  $\theta = 0.324\text{CR} + 0.089$   $r^2 = 0.889$ Count Ratio, CR  
(Actual/Standard)Water Content,  $\theta$   
( $\text{cm}^3/\text{cm}^3$ )

.485

.257

.391

.198

.568

.291

.748

.319

Subsurface, 15-85 cm

Line of Best Fit,  $\theta = 0.419\text{CR} + 0.001$   $r^2 = 0.872$ Count Ratio, CR  
(Actual/Standard)Water Content,  $\theta$   
( $\text{cm}^3/\text{cm}^3$ )

.664

.282

.670

.284

.703

.321

.636

.232

.647

.284

.670

.300

.691

.293

.693

.300

.489

.221

.455

.195

.422

.165

.402

.153

.659

.304

.661

.281

.674

.248

.696

.272

.702

.270

.634

.256

.669

.301

.681

.291

.679

.272

TABLE A-2 (Continued)

<u>Count Ratio, CR</u> <u>(Actual/Standard)</u>	<u>Water Content, <math>\theta</math></u> <u>(<math>\text{cm}^3/\text{cm}^3</math>)</u>
.592	.284
.419	.144
.331	.144
.330	.172
.767	.333
.711	.309
.654	.256

TABLE A-3

Soil Moisture Measured at Different Depths for  
Various Times During Drainage

## Field Measurements of Soil Moisture (Neutron Probe)

Depth (cm)	6h	9h	23h	168h	360h	408h	492h	575h	718h	910h
10	.327	.320	.307	.297	.295	.293	.293	.287	.289	.288
20	.325	.316	.300	.298	.292	.287	.287	.287	.283	.282
30	.357	.328	.318	.304	.292	.292	.285	.286	.282	.271
40	.365	.345	.336	.323	.312	.305	.301	.296	.290	.280
50	.375	.362	.344	.331	.314	.311	.305	.303	.290	.279
60	.375	.365	.348	.337	.314	.302	.297	.292	.277	.269
70	.373	.364	.352	.334	.311	.302	.297	.291	.277	.268
80	.380	.368	.357	.350	.348	.341	.339	.337	.330	.321
90	.380	.368	.360	.360	.361	.355	.356	.355	.354	.346
100	.383	.370	.365	.363	.362	.363	.364	.365	.361	.359
110	.365	.352	.344	.345	.352	.348	.344	.346	.343	.344
120	.374	.352	.354	.347	.348	.346	.345	.350	.342	.339
130	.381	.370	.362	.364	.362	.362	.362	.363	.355	.356
140	.369	.360	.355	.356	.359	.364	.357	.355	.356	.357
150	.359	.424	.352	.347	.348	.350	.349	.351	.343	.348
160	.360	.390	.346	.347	.341	.337	.338	.337	.324	.329
170	.369	.403	.355	.349	.348	.345	.344	.342	.336	.337
175	.370	.381	.356	.344	.348	.346	.344	.344	.342	.339

TABLE A-4  
Soil-water Pressure Head (cmH<sub>2</sub>O) Measured at Different Depths for  
Various Times During Drainage

Field Measurements of Pressure Head		18h	48h	72h	145h	195h	384h	596h	720h	864h	960h
Depth (cm)											
20	100	115	123	151	181	195	213	220	227	229	
30	97	114	122	145	161	186	198	207	211	213	
40	90	106	116	141	155	185	200	207	210	210	
50	85	101	119	140	154	176	188	192	197	199	
60	75	91	109	132	144	167	177	181	184	185	
75		84	95	117	130	153	163	167	170	172	
80	59	80	90	115	126	147	156	161	165	168	
90	35	72	92	104	124	140	143	154	157	160	
110	36	63	68	93	105	143	152	153	155	155	
120	38	65	88	99	121	141	145	151	153	154	
135	30	72	80	115	120	139	148	151	152	153	
140	28	60	76	100	111	133	141	147	149	150	
155	30	57	74	96	108	130	141	145	147	148	
180	30	60	70	99	111	132	141	145	145	145	

TABLE A-5

## Calculation of Hydraulic Conductivity from Field Data

Average Time - 18h	Depth increment (cm)	$d\theta/dt$ (1/day)	$q = \sum z d\theta/dt$ (cm/day)	$dH/dZ$ (cm/cm)	$K = q/dH/dZ$ (cm/day)	$\bar{\theta}$ (cm <sup>3</sup> /cm <sup>3</sup> )	Depth (cm)	
	0-15	$1.967 \times 10^{-2}$	0.295	0.344	0.858	0.3161	10	
	15-25	$1.967 \times 10^{-2}$	0.492	→	1.430	0.3161	20	
	25-35	$1.967 \times 10^{-2}$	0.688		2.001	0.3161	30	
	35-45	$1.102 \times 10^{-2}$	0.799		2.322	0.3449	40	
	45-55	$1.102 \times 10^{-2}$	0.909		2.642	0.3449	50	
	55-65	$1.836 \times 10^{-2}$	1.092		3.176	0.3485	60	
	65-75	$1.836 \times 10^{-2}$	1.276		3.709	0.3485	70	
	75-85	$1.574 \times 10^{-2}$	1.433		4.166	0.3639	80	
	85-95	$1.77 \times 10^{-2}$	1.610		4.680	0.3655	90	
	95-105	$1.495 \times 10^{-3}$	1.760		5.116	0.3689	100	
	105-125	$7.869 \times 10^{-3}$	1.838		5.343	0.3549	110, 120	
	125-135	$1.062 \times 10^{-2}$	1.945		0.892	2.180	0.3666	130
	135-145	$9.840 \times 10^{-3}$	2.043		→	2.290	0.3592	140
	145-155	$5.902 \times 10^{-3}$	2.102			2.356	0.3521	150
	155-165	$3.93 \times 10^{-3}$	2.142			2.401	0.3441	160
	165-175	$7.869 \times 10^{-3}$	2.220			2.489	0.3584	170
	175-185	$1.259 \times 10^{-2}$	2.346		2.463	0.3613	180	

TABLE A-5 (Continued)

Average Time - 48h	Depth Increment (cm)	$d\theta/dt$ (l/day)	$q = \int z d\theta/dt$ (cm/day)	$dH/dZ$ (cm/cm)	$K=q/dH/dZ$ (cm/day)	$\theta$ (cm <sup>3</sup> /cm <sup>3</sup> )	Depth (cm)
	0-15	$4.721 \times 10^{-3}$	0.0708	0.351	0.202	0.3090	10
	15-25	$4.721 \times 10^{-3}$	0.1180		0.336	0.2090	20
	25-35	$4.721 \times 10^{-3}$	0.1652		0.471	0.3090	30
	35-45	$4.000 \times 10^{-3}$	0.2052		0.585	0.3400	40
	45-55	$4.000 \times 10^{-3}$	0.2452		0.699	0.3400	50
	55-65	$3.93 \times 10^{-3}$	0.2845		0.810	0.3439	60
	65-75	$3.93 \times 10^{-3}$	0.3238		0.922	0.3439	70
	75-85	$4.721 \times 10^{-3}$	0.3710		1.060	0.3554	80
	85-95	$1.784 \times 10^{-3}$	0.3888		1.108	0.3634	90
	95-105	$1.888 \times 10^{-3}$	0.4077		1.162	0.3665	100
	105-125	$4.197 \times 10^{-4}$	0.4119		0.923	0.3495	110, 120
	125-135	$3.147 \times 10^{-3}$	0.4434		0.4804	0.3633	130
	135-145	$2.317 \times 10^{-5}$	0.4436		0.4806	0.3347	140
	145-155	$1.639 \times 10^{-4}$	0.4453		0.4806	0.3369	150
	155-165	$2.373 \times 10^{-4}$	0.4476		0.4832	0.3369	160
	165-175	$4.434 \times 10^{-4}$	0.4521		0.4876	0.3525	170
	175-185	$3.35 \times 10^{-4}$	0.4559		0.4921	0.3528	180

TABLE A-5 (Continued)

Average Time - 145 h											
Depth Increment (cm)	$d\theta/dt$ (1/day)	$q = \sum z d\theta/dt$ (cm/day)	$dH/dZ$ (cm/cm)	$K=q/dH/dZ$ (cm/day)	$\theta$ (cm <sup>3</sup> /cm <sup>3</sup> )	Depth (cm)					
0-15	$2.754 \times 10^{-3}$	0.0412	0.274	0.150	0.2957	10					
15-25	$2.754 \times 10^{-3}$	0.0687	↓	0.251	0.2957	20					
25-35	$2.754 \times 10^{-3}$	0.0962		0.351	0.2957	30					
35-45	$2.72 \times 10^{-3}$	0.1234		0.450	0.3271	40					
45-55	$2.72 \times 10^{-3}$	0.1506		0.550	0.3271	50					
55-65	$2.52 \times 10^{-3}$	0.1758		0.642	0.3344	60					
65-75	$2.52 \times 10^{-3}$	0.2016		0.736	0.3344	70					
75-85	$8.544 \times 10^{-4}$	0.2095		0.765	0.3502	80					
85-95	$1.500 \times 10^{-3}$	0.2245		0.819	0.3620	90					
95-105	$1.299 \times 10^{-4}$	0.2258		0.824	0.3646	100					
105-125	$1.23 \times 10^{-4}$	0.2270		1.000	0.2270	0.3485	110, 120				
125-135	$1.23 \times 10^{-4}$	0.2283	↓	0.2283	0.3626	130					
135-145	$2.317 \times 10^{-5}$	0.2285		0.2285	0.3570	140					
145-155	$1.639 \times 10^{-4}$	0.2302		0.2302	0.3498	150					
155-165	$2.373 \times 10^{-4}$	0.2325		0.2325	0.3359	160					
165-175	$4.43 \times 10^{-4}$	0.2370		0.2370	0.3508	170					
175-185	$3.85 \times 10^{-4}$	0.2408		0.2408	0.3513	180					

TABLE A-5 (Continued)

Average Time - 384h

Depth Increment (cm)	$d\theta/dt$ (1/day)	$q = \sum z d\theta/dt$ (cm/day)	$dH/dZ$ (cm/cm)	$K = q/dH/dZ$ (cm/day)	$\theta$ ( $cm^3/cm^3$ )	Depth (cm)
0-15	$5.04 \times 10^{-4}$	0.00756	0.230	0.0329	0.2908	10
15-25	$5.04 \times 10^{-4}$	0.0126	↓	0.0548	0.2908	20
25-35	$5.04 \times 10^{-4}$	0.0176		0.0756	0.2908	30
35-45	$1.73 \times 10^{-3}$	0.0349	↓	0.1520	0.3082	40
45-55	$1.73 \times 10^{-3}$	0.0522		0.2270	0.3082	50
55-65	$2.361 \times 10^{-3}$	0.0758	↓	0.3300	0.3310	60
65-75	$2.361 \times 10^{-3}$	0.0994		0.4320	0.3310	70
75-85	$1.574 \times 10^{-3}$	0.1151	↓	0.5000	0.3410	80
85-95	$1.259 \times 10^{-4}$	0.1277		0.555	0.3574	90
95-105	$1.299 \times 10^{-4}$	0.1290	0.860	0.1500	0.3533	100
105-125	$1.230 \times 10^{-4}$	0.1302	↓	0.1513	0.3479	110, 120
125-135	$1.230 \times 10^{-4}$	0.1315		0.1529	0.3601	130
135-145	$2.317 \times 10^{-5}$	0.1317	↓	0.2657	0.3482	140
145-155	$1.639 \times 10^{-4}$	0.1333		0.155	0.3482	150
155-165	$2.373 \times 10^{-4}$	0.1357	↓	0.1578	0.3336	160
165-175	$4.434 \times 10^{-4}$	0.1402		0.1630	0.3465	170
175-185	$3.850 \times 10^{-4}$	0.1440		0.1674	0.3474	180



TABLE A-5 (Continued)

Average Time - 720h											
Depth Increment (cm)	$d\theta/dt$ (1/day)	$q = \sum z d\theta/dt$ (cm/day)	$dH/dZ$ (cm/cm)	$K = q/dH/dZ$ (cm/day)	$\theta$ ( $cm^3/cm^3$ )	Depth (cm)					
0-15	$3.279 \times 10^{-4}$	$4.918 \times 10^{-3}$	0.164	0.0300	0.2850	10					
15-25	$3.279 \times 10^{-4}$	$8.198 \times 10^{-3}$	↓	0.0500	0.2850	20					
25-35	$3.279 \times 10^{-4}$	$1.148 \times 10^{-2}$		0.0700	0.2850	30					
35-45	$3.200 \times 10^{-4}$	$1.468 \times 10^{-2}$	↓	0.0895	0.2872	40					
45-55	$3.200 \times 10^{-4}$	$1.788 \times 10^{-2}$		0.1090	0.2872	50					
55-65	$1.967 \times 10^{-4}$	$1.984 \times 10^{-2}$	↓	0.1210	0.2758	60					
65-75	$1.967 \times 10^{-4}$	$2.181 \times 10^{-2}$		0.1330	0.2758	70					
75-85	$1.729 \times 10^{-3}$	$3.910 \times 10^{-2}$	↓	0.2380	0.3269	80					
85-95	$5.200 \times 10^{-4}$	$4.430 \times 10^{-2}$		0.0515	0.3510	90					
95-105	$1.300 \times 10^{-4}$	$4.560 \times 10^{-2}$	0.860	0.0535	0.3615	100					
105-125	$1.200 \times 10^{-4}$	$4.680 \times 10^{-2}$	↓	0.0544	0.3456	110, 120					
125-135	$0.000 \times 10^{-4}$	$4.680 \times 10^{-2}$		0.0468	0.3590	130					
135-145	$2.317 \times 10^{-5}$	$4.700 \times 10^{-2}$	↓	0.05465	0.3566	140					
145-155	$1.639 \times 10^{-4}$	$4.870 \times 10^{-2}$		0.0566	0.3459	150					
155-165	$2.373 \times 10^{-4}$	$5.100 \times 10^{-2}$	↓	0.0593	0.3303	160					
165-175	$4.434 \times 10^{-4}$	$5.550 \times 10^{-2}$		0.0645	0.3404	170					
175-185	$3.850 \times 10^{-4}$	$5.930 \times 10^{-2}$		0.0689	0.3420	180					

TABLE A-5 (Continued)


Average Time - 910h												
Depth Increment (cm)	$d\theta/dt$ (1/day)	$q = \int z d\theta/dt$ (cm/day)	$dH/dZ$ (cm/cm)	$K = q/dH/dZ$ (cm/day)	$\theta$ ( $cm^3/cm^3$ )	Depth (cm)						
0-15	$1.049 \times 10^{-4}$	$1.573 \times 10^{-3}$	0.164	0.00959	0.2826	10						
15-25	$1.049 \times 10^{-4}$	$2.622 \times 10^{-3}$	 0.860	0.01599	0.2826	20						
25-35	$1.049 \times 10^{-4}$	$3.671 \times 10^{-3}$		0.04091	0.2826	30						
35-45	$4.720 \times 10^{-4}$	$8.393 \times 10^{-3}$		0.0512	0.2820	40						
45-55	$4.720 \times 10^{-4}$	$8.864 \times 10^{-3}$		0.05405	0.2820	50						
55-65	$1.570 \times 10^{-4}$	$9.022 \times 10^{-3}$		0.05501	0.2687	60						
65-75	$1.570 \times 10^{-4}$	$9.180 \times 10^{-3}$		0.05598	0.2687	70						
75-85	$4.720 \times 10^{-4}$	$1.390 \times 10^{-2}$		0.08476	0.3226	80						
85-95	$3.279 \times 10^{-4}$	$1.720 \times 10^{-2}$		0.10488	0.3419	90						
95-105	$1.299 \times 10^{-4}$	.0185		0.0215	0.3602	100						
105-125	$1.230 \times 10^{-4}$	$1.970 \times 10^{-2}$		0.0229	0.3443	110, 120						
125-135	$1.230 \times 10^{-4}$	$2.090 \times 10^{-2}$		0.0209	0.3574	130						
135-145	$2.317 \times 10^{-4}$	$2.113 \times 10^{-2}$		0.02457	0.3563	140						
145-155	$1.639 \times 10^{-4}$	$2.278 \times 10^{-2}$		0.0265	0.3442	150						
155-165	$2.373 \times 10^{-4}$	$2.514 \times 10^{-2}$		0.0292	0.3279	160						
165-175	$4.434 \times 10^{-4}$	$2.957 \times 10^{-2}$		0.0344	0.3360	170						
175-185	$3.850 \times 10^{-4}$	$3.342 \times 10^{-2}$		0.0389	0.3382	180						

TABLE A-6

Water Retentivity Values of Pressure Potential and  
Water Content Used in the Calculation  
of Hydraulic Conductivity

## Laboratory Data

Surface, 0-15 cm  $\theta_s = 0.39 \text{ cm}^3/\text{cm}^3$

$h_i$ (kPa)	$\theta_i$ ( $\text{cm}^3/\text{cm}^3$ )	$K_g=4.25\text{cm/day}$	$K_s=20\text{cm/day}$	$K_s=30\text{cm/day}$
		$K_i$ ( $\text{cm/day}$ )	$K_i$ ( $\text{cm/day}$ )	$K_i$ ( $\text{cm/day}$ )
10.7	0.39	$4.25 \times 10^0$	$2.000 \times 10^1$	$3.000 \times 10^1$
13.0	0.38	$2.60 \times 10^0$	$1.223 \times 10^1$	$1.835 \times 10^1$
16.2	0.37	$1.60 \times 10^0$	$7.529 \times 10^0$	$1.129 \times 10^1$
20.0	0.36	$-9.33 \times 10^{-1}$	$4.390 \times 10^0$	$6.586 \times 10^0$
25.5	0.35	$5.46 \times 10^{-1}$	$2.569 \times 10^0$	$3.854 \times 10^0$
32.0	0.34	$-3.15 \times 10^{-1}$	$1.482 \times 10^0$	$2.223 \times 10^0$
41.0	0.33	$-1.78 \times 10^{-1}$	$8.376 \times 10^{-1}$	$1.256 \times 10^0$
52.0	0.32	$9.80 \times 10^{-2}$	$4.612 \times 10^{-1}$	$6.918 \times 10^{-1}$
66.0	0.31	$5.20 \times 10^{-2}$	$2.447 \times 10^{-1}$	$3.671 \times 10^{-1}$
88.0	0.30	$2.68 \times 10^{-2}$	$1.261 \times 10^{-1}$	$1.892 \times 10^{-1}$
115.0	0.29	$1.33 \times 10^{-2}$	$6.259 \times 10^{-2}$	$9.388 \times 10^{-2}$
155.0	0.28	$6.20 \times 10^{-3}$	$2.918 \times 10^{-2}$	$4.365 \times 10^{-2}$
215.0	0.27	$2.70 \times 10^{-3}$	$1.270 \times 10^{-2}$	$1.906 \times 10^{-2}$
300.0	0.26	$1.10 \times 10^{-3}$	$5.176 \times 10^{-3}$	$7.765 \times 10^{-3}$
450.0	0.25	$3.76 \times 10^{-4}$	$1.769 \times 10^{-3}$	$2.654 \times 10^{-3}$
660.0	0.24	$8.86 \times 10^{-7}$	$4.169 \times 10^{-6}$	$6.254 \times 10^{-6}$

## Laboratory data

Subsurface, 15-55 cm  $\theta_s = 0.45 \text{ cm}^3/\text{cm}^3$

$K_s = 40.9 \text{ cm/day}$

$h_i$ (kPa)	$\theta_i$ ( $\text{cm}^3/\text{cm}^3$ )	$K_i$ ( $\text{cm}^3/\text{cm}^3$ )
11.2	0.45	$4.09 \times 10^1$
14.2	0.43	$3.08 \times 10^1$
15.1	0.41	$2.28 \times 10^1$
17.0	0.39	$1.69 \times 10^1$
18.8	0.37	$1.22 \times 10^1$
20.7	0.35	$8.69 \times 10^0$
22.3	0.33	$5.98 \times 10^0$

TABLE A-6 (Continued)

$h_i$ (kPa)	$K_s=40.9\text{cm/day}$	
	$\theta_i$ ( $\text{cm}^3/\text{cm}^3$ )	$K_i$ ( $\text{cm/day}$ )
24.2	0.31	$4.04 \times 10^0$
26.4	0.29	$2.59 \times 10^0$
29.5	0.27	$1.62 \times 10^0$
33.1	0.25	$-9.54 \times 10^{-1}$
35.5	0.23	$-5.11 \times 10^{-1}$
44.0	0.21	$-2.55 \times 10^{-1}$
54.0	0.19	$-1.13 \times 10^{-1}$
70.0	0.17	$2.00 \times 10^{-2}$
99.0	0.15	$1.44 \times 10^{-2}$
152.0	0.13	$3.74 \times 10^{-3}$
270.0	0.11	$6.10 \times 10^{-4}$
830.0	0.09	$3.97 \times 10^{-5}$

## Laboratory Data

Subsurface, 55-90 cm  $\theta_s = 0.45 \text{ cm}^3/\text{cm}^3$ 

$h_i$ (kPa)	$K_s=53.4\text{cm/day}$	
	$\theta_i$ ( $\text{cm}^3/\text{cm}^3$ )	$K_i$ ( $\text{cm/day}$ )
11.0	0.43	$4.01 \times 10^1$
12.0	0.41	$2.96 \times 10^1$
13.0	0.39	$2.14 \times 10^1$
14.0	0.37	$6.52 \times 10^1$
15.0	0.35	$1.04 \times 10^1$
16.2	0.33	$6.98 \times 10^0$
17.8	0.31	$4.50 \times 10^0$
19.6	0.29	$2.78 \times 10^0$
21.8	0.27	$1.63 \times 10^0$
25.6	0.25	$8.97 \times 10^{-1}$
28.2	0.23	$-4.47 \times 10^{-1}$
33.0	0.21	$1.99 \times 10^{-1}$
40.0	0.19	$7.70 \times 10^{-2}$
54.0	0.17	$2.60 \times 10^{-2}$
78.0	0.15	$7.34 \times 10^{-3}$
122.0	0.13	$1.70 \times 10^{-3}$
220.0	0.11	$3.38 \times 10^{-4}$

TABLE A-6 (Continued)

$h_i$ (kPa)	$\theta_i$ ( $\text{cm}^3/\text{cm}^3$ )	$K_s=53.4$ cm/day
		$K_i$ (cm/day)
440.0	0.09	$6.60 \times 10^{-5}$
1100.0	0.07	$1.10 \times 10^{-5}$
1350.0	0.05	

Combined Laboratory and Field Data  
Surface, 0-20 cm  $\theta_s = 0.39 \text{ cm}^3/\text{cm}^3$

$h_i$ (kPa)	$\theta_i$ ( $\text{cm}^3/\text{cm}^3$ )	$K_s=4.25$ cm/day	$K_s=20$ cm/day	$K_s=30$ cm/day
		$K_i$ (cm/day)	$K_i$ (cm/day)	$K_i$ (cm/day)
1.10	0.39	4.25		
1.28	0.38	2.58		
1.55	0.37	1.50	$7.06 \times 10^0$	$1.01 \times 10^1$
1.85	0.36	$8.24 \times 10^{-1}$	$3.88 \times 10^0$	$5.82 \times 10^0$
2.35	0.35	$4.24 \times 10^{-1}$		
2.90	0.34	$2.00 \times 10^{-1}$	$1.99 \times 10^0$	$2.99 \times 10^0$
3.90	0.33	$8.27 \times 10^{-2}$	$9.41 \times 10^{-1}$	$1.41 \times 10^0$
5.60	0.32	$2.90 \times 10^{-2}$	$3.89 \times 10^{-1}$	$5.83 \times 10^{-1}$
8.00	0.31	$7.50 \times 10^{-3}$	$1.36 \times 10^{-1}$	$2.04 \times 10^{-1}$
18.00	0.30	$9.59 \times 10^{-4}$	$3.53 \times 10^{-2}$	$5.29 \times 10^{-2}$
180.00	0.29	$4.00 \times 10^{-5}$	$4.52 \times 10^{-3}$	$6.78 \times 10^{-3}$
290.0	0.28			
420.0	0.27			
580.0	0.26			
760.0	0.25			
920.0	0.24			

Combined Laboratory and Field Data  
Subsurface, 15-55 cm  $\theta_s = 0.45 \text{ cm}^3/\text{cm}^3$

$h_i$ (kPa)	$\theta_i$ ( $\text{cm}^3/\text{cm}^3$ )	$K_s=40.9$ cm/day
		$K_i$ (cm/day)
1.30	0.45	$4.09 \times 10^1$
2.20	0.43	$1.81 \times 10^1$

TABLE A-6 (Continued)

$h_i$ (kPa)	$\theta_i$ (cm <sup>3</sup> /cm <sup>3</sup> )	$K_s=40.9$ cm/day
		$K_i$ (cm/day)
3.30	0.41	$8.77 \times 10^0$
4.90	0.39	$4.60 \times 10^0$
7.00	0.37	$2.54 \times 10^0$
9.80	0.35	$1.49 \times 10^0$
13.50	0.33	$9.01 \times 10^{-1}$
17.00	0.31	$5.53 \times 10^{-1}$
21.00	0.29	$3.31 \times 10^{-1}$
25.00	0.27	$1.96 \times 10^{-1}$
29.50	0.25	$1.11 \times 10^{-1}$
35.50	0.23	$5.80 \times 10^{-2}$
44.00	0.21	$2.90 \times 10^{-2}$
54.00	0.19	$1.29 \times 10^{-2}$
70.00	0.17	$5.13 \times 10^{-3}$
99.00	0.15	$1.66 \times 10^{-3}$
152.00	0.13	$4.17 \times 10^{-4}$
270.00	0.11	$6.90 \times 10^{-5}$
830.00	0.09	$4.50 \times 10^{-6}$

Combined Laboratory and Field Data

Subsurface, 55-90 cm  $\theta_s = 0.45$  cm<sup>3</sup>/cm<sup>3</sup>

$h_i$ (kPa)	$\theta_i$ (cm <sup>3</sup> /cm <sup>3</sup> )	$K_s=53.40$ cm/day
		$K_i$ (cm/day)
1.30	0.45	$5.34 \times 10^1$
2.20	0.43	$2.36 \times 10^1$
3.30	0.41	$1.15 \times 10^1$
4.90	0.39	$6.05 \times 10^0$
7.00	0.37	$3.36 \times 10^0$
9.80	0.35	$1.98 \times 10^0$
13.50	0.33	$1.20 \times 10^0$
17.00	0.31	$7.45 \times 10^{-1}$
21.00	0.29	$4.50 \times 10^{-1}$
25.00	0.27	$2.69 \times 10^{-1}$
29.00	0.25	$1.53 \times 10^{-1}$
35.50	0.23	$8.10 \times 10^{-2}$

TABLE A-6 (Continued)

$h_i$ (kPa)	$\theta_i$ ( $\text{cm}^3/\text{cm}^3$ )	$K_s=53.40\text{cm/day}$ $K_i$ ( $\text{cm/day}$ )
44.00	0.21	$4.00 \times 10^{-2}$
54.00	0.19	$1.80 \times 10^{-2}$
69.00	0.17	$7.60 \times 10^{-3}$
92.20	0.15	$2.60 \times 10^{-3}$
148.00	0.13	$7.20 \times 10^{-4}$
250.00	0.11	$1.53 \times 10^{-4}$

TABLE A-7

Double-Tube Data Used for Calculation  
of  $K_s$

	Outer-Tube Constant		Equal Levels	
	<u>H<sub>1</sub> (cm)</u>	<u>t (min)</u>	<u>H<sub>1</sub> (cm)</u>	<u>t (min)</u>
5 cm depth	0.00	0	0.0	0
Rv = 2.54 cm	0.20	15	0.1	10
Rc = 6.67 cm	0.35	25	0.3	18
d = 5 cm	0.55	39	0.5	31
F = 0.75	0.80	56	0.8	52
	1.10	74	1.1	69
			1.3	85
40 cm depth	4	0.9	5	1.3
Rv = 2.54 cm	11	3.1	8	2.1
Rc = 6.67 cm	15	4.5	12	3.5
d = 3 cm	20	6.0	15	4.0
F = 1.10	25	8.0	20	5.4
	30	9.6	25	6.8
			30	8.25
			35	9.70
70 cm depth	5	1.4	5	1.3
Rv = 2.54 cm	8	2.3	8	2.0
Rc = 6.67 cm	12	3.5	13	3.0
d = 3 cm	15	4.5	15	4.0
F = 1.10	20	6.2	20	5.5
	25	8.0	25	6.8
	30	9.9	30	8.25
	35	12.1	35	9.70



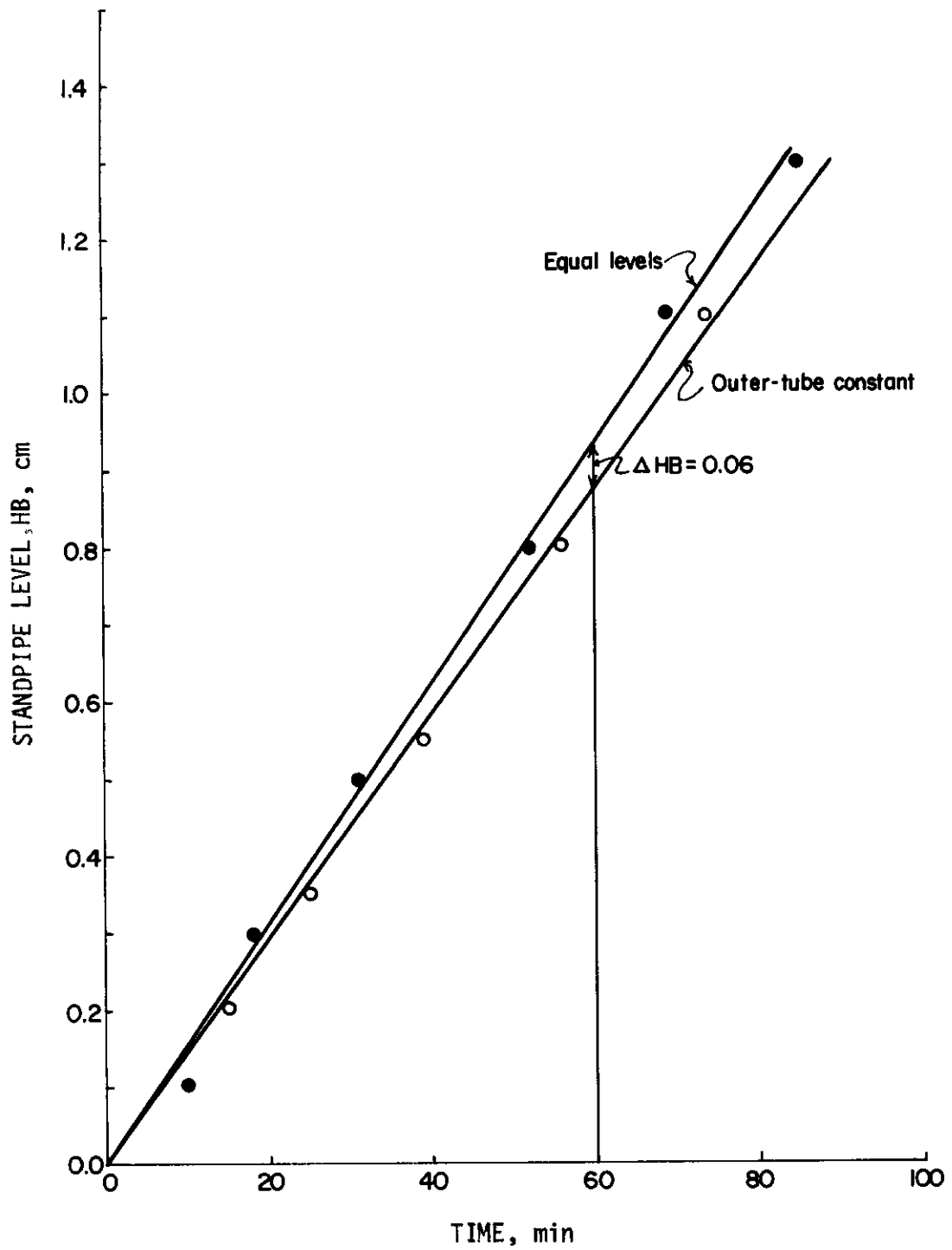


Fig. A-1. Double-tube data for 5 cm depth.

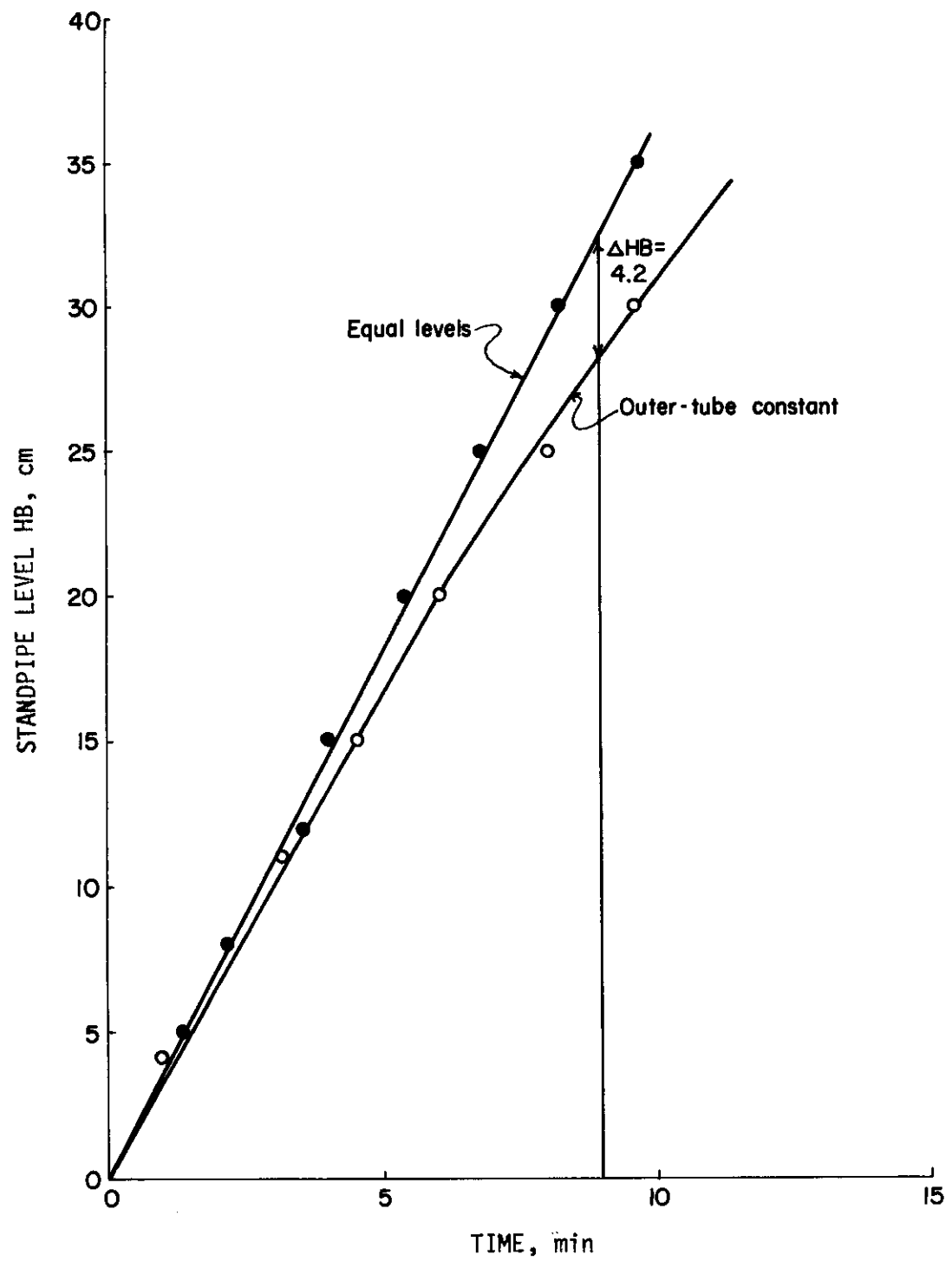


Fig. A-2. Double-tube data for 40 cm depth.

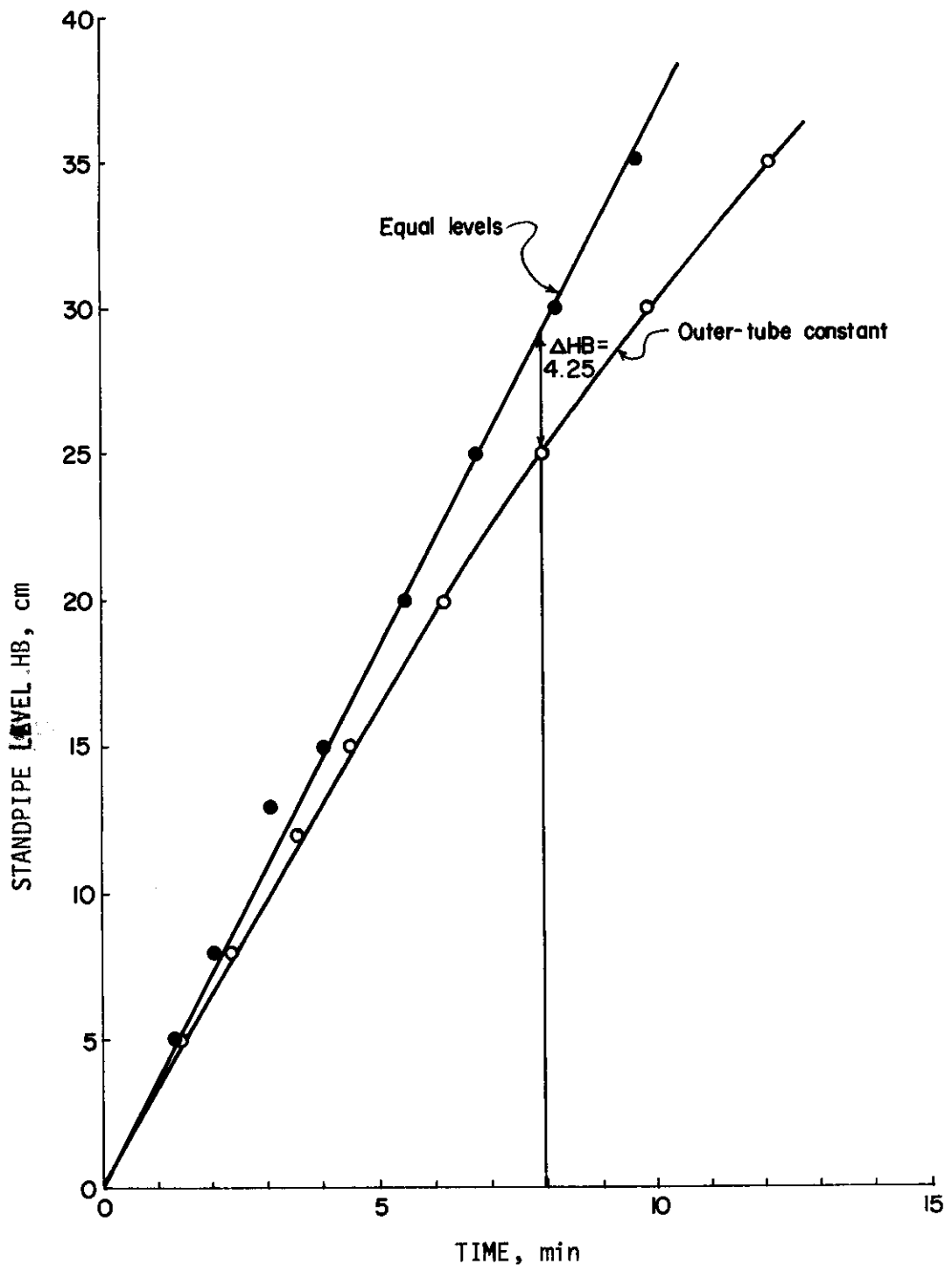


Fig. A-3. Double-tube data for 70 cm depth.

TABLE A-8

## Centrifuge Data

Core #	Depth (cm)	2m+L (cm)	L (cm)	$\omega$ (1/sec)	$R_1(\infty) - R_1(o)$ (g)	D (cm <sup>2</sup> /min)	K (cm/day)	$\phi$ (cm <sup>3</sup> /cm <sup>3</sup> )
1	30	30.9	6	62.832	0.155	0.900	0.200	0.301
2	42-52	30.9	6	62.832	0.190	0.700	0.181	0.291
3	30	30.9	6	83.771	0.330	0.350	0.258	0.301
3a	50-60	28.5	6	73.304	0.040	0.425	0.099	0.272
3b	50-60	28.5	6	83.771	0.30	0.220	0.129	0.272
4	65-75	28.5	6	78.540	0.275	0.425	0.099	0.284
6	80	31.7	6	78.540	0.042	0.700	0.0277	0.253
7	35-55	30.9	6	86.394	0.330	0.500	0.129	0.144
9	65-85	30.9	6	83.771	0.390	0.35	0.1068	0.172
11	15-25	31.6	6	83.771	0.70	0.172	0.177	0.333
12	25-45	31.6	6	83.776	0.12	0.60	0.0594	0.301